VASCULAR ATP-SENSITIVE POTASSIUM CHANNELS IMPACT SPATIAL AND TEMPORAL OXYGEN TRANSPORT: IMPLICATIONS FOR SULPHONYLUREA THERAPY

by

CLARK THOMAS HOLDSWORTH

B.S., State University of New York at Cortland, 2009
M.S., Kansas State University, 2013

AN ABSTRACT OF A DISSERTATION

submitted in partial fulfillment of the requirements for the degree

DOCTOR OF PHILOSOPHY

Department of Anatomy and Physiology
College of Veterinary Medicine

KANSAS STATE UNIVERSITY
Manhattan, Kansas

2015

Abstract

Matching local muscle O_2-supply to O_2-demand during the prodigious exercise-induced metabolic challenge is achieved through coordinated mechanisms of vascular control. The unique sensitivity of ATP-sensitive potassium (K_{ATP}) channels to cell metabolism indicates the potential to match energetic demand to peripheral O_2 transport. The aim of this dissertation was to determine the magnitude and kinetics of the K_{ATP} channel contribution to vascular control during exercise in health and heart failure. It was hypothesized that K_{ATP} channel inhibition via glibenclamide would, in healthy rats, 1) reduce exercising skeletal muscle blood flow and vascular conductance 2) speed the fall of microvascular O_2 driving pressure (PO_2mv; set by the O_2 delivery-O_2 utilization ratio) during muscle contractions and 3) in heart failure rats, augment the PO_2mv undershoot and delay the time to reach the contracting steady-state. A total of 55 male Sprague-Dawley rats were used under control and glibenclamide conditions (5 mg kg^{-1}). Hindlimb muscle blood flow (radiolabelled microspheres) was determined at rest (n = 6) or during treadmill exercise (n = 6-8; 20, 40 and 60 m min^{-1}, 5% incline). Spinotrapezius muscle PO_2mv (phosphorescence quenching) was measured in 16 heart failure (coronary artery ligation) and 12 healthy rats and during 180 s of 1-Hz twitch contractions (~6 V). The major effects of glibenclamide were, in healthy rats, 1) a reduction in exercising hindlimb skeletal muscle blood flow with the greatest effect in predominantly oxidative muscle fiber types and at higher running speeds 2) an increased prevalence of the undershoot of PO_2mv steady-state and doubled time to reach the steady-state and 3) in heart failure rats, a reduced baseline PO_2mv, an augmented undershoot of the steady-state and time to reach steady-state and a reduction in the mean PO_2mv during contractions. These data suggest that the K_{ATP} channel contributes substantially to exercise-induced hyperemia and may contribute to the slowing of $\dot{V}O_2$ kinetics given the spatial

and temporal effects of glibenclamide. The K_{ATP} channel-mediated protection against a severe O_2-delivery to O_2-utilization mismatch at the onset of contractions raises serious concerns for sulphonylurea treatment in diabetes which is likely to cause perturbations of [metabolite] and compromise exercise tolerance.

VASCULAR ATP-SENSITIVE POTASSIUM CHANNELS IMPACT SPATIAL AND TEMPORAL OXYGEN TRANSPORT: IMPLICATIONS FOR SULPHONYLUREA THERAPY

by

CLARK THOMAS HOLDSWORTH

B.S., State University of New York at Cortland, 2009
M.S., Kansas State University, 2013

A DISSERTATION

submitted in partial fulfillment of the requirements for the degree

DOCTOR OF PHILOSOPHY

Department of Anatomy and Physiology
College of Veterinary Medicine

KANSAS STATE UNIVERSITY
Manhattan, Kansas

2015

Approved by:

Major Professor
Dr. Timothy I. Musch

Copyright

Abstract

Matching local muscle O_2-supply to O_2-demand during the prodigious exercise-induced metabolic challenge is achieved through coordinated mechanisms of vascular control. The unique sensitivity of ATP-sensitive potassium (K_{ATP}) channels to cell metabolism indicates the potential to match energetic demand to peripheral O_2 transport. The aim of this dissertation was to determine the magnitude and kinetics of the K_{ATP} channel contribution to vascular control during exercise in health and heart failure. It was hypothesized that K_{ATP} channel inhibition via glibenclamide would, in healthy rats, 1) reduce exercising skeletal muscle blood flow and vascular conductance 2) speed the fall of microvascular O_2 driving pressure (PO_2mv; set by the O_2 delivery-O_2 utilization ratio) during muscle contractions and 3) in heart failure rats, augment the PO_2mv undershoot and delay the time to reach the contracting steady-state. A total of 55 male Sprague-Dawley rats were used under control and glibenclamide conditions (5 mg kg^{-1}). Hindlimb muscle blood flow (radiolabelled microspheres) was determined at rest (n = 6) or during treadmill exercise (n = 6-8; 20, 40 and 60 m min^{-1}, 5% incline). Spinotrapezius muscle PO_2mv (phosphorescence quenching) was measured in 16 heart failure (coronary artery ligation) and 12 healthy rats and during 180 s of 1-Hz twitch contractions (~6 V). The major effects of glibenclamide were, in healthy rats, 1) a reduction in exercising hindlimb skeletal muscle blood flow with the greatest effect in predominantly oxidative muscle fiber types and at higher running speeds 2) an increased prevalence of the undershoot of PO_2mv steady-state and doubled time to reach the steady-state and 3) in heart failure rats, a reduced baseline PO_2mv, an augmented undershoot of the steady-state and time to reach steady-state and a reduction in the mean PO_2mv during contractions. These data suggest that the K_{ATP} channel contributes substantially to exercise-induced hyperemia and may contribute to the slowing of $\dot{V}O_2$ kinetics given the spatial

and temporal effects of glibenclamide. The K_{ATP} channel-mediated protection against a severe O_2-delivery to O_2-utilization mismatch at the onset of contractions raises serious concerns for sulphonylurea treatment in diabetes which is likely to cause perturbations of [metabolite] and compromise exercise tolerance.

Table of Contents

List of Figures

List of Tables

Dedication

Dedicated to my loving parents William and Marcia Holdsworth, my brother Neil Holdsworth and the memory of my cousin Lauren Miller.

Chapter 1 - Background

Noma et al. first demonstrated the presence of K_{ATP} channels in cardiac myocytes over three decades ago (Noma, 1983). In cardiac myocytes they were able to measure a K^+ efflux that was sensitive to both the application of ATP and ADP. However, K_{ATP} channel research is most commonly associated with the channel function in pancreatic beta cells (Ashcroft et al., 1984). The discovery that K_{ATP} channels could couple glucose-induced metabolism increases to insulin release led directly to the pharmacological progress underlying the treatment of diabetes mellitus. The early realization of the potential for K_{ATP} channel exploitation in diabetes mellitus was foundational to the multi-fold increase in the search for channel activators and inhibitors. Inhibitors ranged widely from first generation tolbutamide to the recent use of the sulphonlyureas glipizide and glibenclamide. The channel activators are diverse and include the benzothiadiazine, diazoxide, and the cyanoguanidine, pinacidil. The differences in function appear to be related to a varying affinity for the diverse isoforms of K_{ATP} channel proteins (Quast et al., 1994).

The structure and function of the K_{ATP} channel is complex and not completely understood. I will limit the subsequent discussion to the characteristics of the vascular K_{ATP} channel. Each K_{ATP} channel consists of the four pore forming units Kir6.1 and the four subunits SUR2B. The pore forming unit appears to be the main site for the binding of 4 ATP molecules independently and non-cooperatively which results in steep inhibitory dependence and can be achieved with non-hydrolyzable analogs suggesting that the energy from ATP hydrolysis is not requisite for channel inhibition. The pore tetramer is a standard K^+ inward rectifier which consists of two transmembrane helical domains, TMD1 and TMD2, and cytoplasmic NH_2 and COOH termini. The four SUR2B subunits are ATP binding cassette proteins arranged in a

heteromeric octamer with the Kir6.1 pore forming units. Pinacidil is a potent activator of the SUR2 isoforms compared to diazoxide which targets SUR1.

The first instances of K_{ATP} channel block in vascular smooth muscle were observed by Nelson and colleagues in 1990 in rabbit mesenteric arteries (Nelson et al., 1990). The results were expanded to demonstrate vascular depolarization, vasoconstriction, and attenuated functional sympatholysis during K_{ATP} channel block (Beech et al., 1993; Mori et al., 1995; Thomas et al., 1997). Within the field of exercise physiology these investigations were transitioned to skeletal muscle vascular beds. K_{ATP} channel block was shown to reduce the forearm hyperemic response to ischemia (Banitt et al., 1996; Bijlstra et al., 1996a). The response could also be augmented by K_{ATP} channel activation suggesting that human forearm muscle contains a recruitable pool of K_{ATP} channels (Bank et al., 2000.; Bijlstra et al., 1996b).

The standard practiceof sulphonlyurea treatment clinically has resulted in unintended consequences. Despite the effectiveness in combating hyperglycemia there appears to be an increased risk of cardiovascular mortality and morbidity with sulphonlyurea therapy (Fadini et al., 2015; Larsen et al., 1999; Morgan et al., 2014; Simpson et al., 2006). This may result from the effects of vascular K_{ATP} channel inhibition as described above. The extent of these issues has led the American College of Physicians to recommend that sulphonylureas be prescribed only in diabetes cases where diet, exercise and the hyperglycemia regulator metformin are not effective (Qaseem et al., 2012).

References

Ashcroft, F.M., Harrison, D.E., Ashcroft, S.J., 1984. Glucose induces closure of single potassium channels in isolated rat pancreatic beta-cells. Nature 312, 446–448.

Banitt, P.F., Smits, P., Williams, S.B., Ganz, P., Creager, M.A., 1996. Activation of ATP-sensitive potassium channels contributes to reactive hyperemia in humans. Am. J. Physiol. 271, H1594–H1598.

Bank, A.J., Sih, R., Mullen, K., Osayamwen, M., Lee, P.C., 2000. Vascular ATP-Dependent Potassium Channels, Nitric Oxide, and Human Forearm Reactive Hyperemia. Cardiovasc. Drugs Ther. 14, 23–29.

Beech, D.J., Zhang, H., Nakao, K., Bolton, T.B., 1993. K channel activation by nucleotide diphosphates and its inhibition by glibenclamide in vascular smooth muscle cells. Br. J. Pharmacol. 110, 573–582.

Beech, D.J., Zhang, H., Nakao, K., Bolton, T.B., 1993. Single channel and whole-cell K-currents evoked by levcromakalim in smooth muscle cells from the rabbit portal vein. Br. J. Pharmacol. 110, 583–590.

Bijlstra, P.J., den Arend, J.A., Lutterman, J.A., Russel, F.G., Thien, T., Smits, P., 1996a. Blockade of vascular ATP-sensitive potassium channels reduces the vasodilator response to ischaemia in humans. Diabetologia 39, 1562–1568.

Bijlstra, P.J., Lutterman, J.A., Russel, F.G., Thien, T., Smits, P., 1996b. Interaction of sulphonylurea derivatives with vascular ATP-sensitive potassium channels in humans. Diabetologia 39, 1083–1090.

Fadini, G.P., Avogaro, A., Degli Esposti, L., Russo, P., Saragoni, S., Buda, S., Rosano, G., Pecorelli, S., Pani, L., Martinetti, S., Mero, P., Raeli, L., Migliazza, S., Dellagiovanna, M., Cerra, C., Gambera, M., Piccinelli, R., Zambetti, M., Atzeni, F., Valsecchi, V., DeLuca, P., Scopinaro, E., Moltoni, D., Pini, E., Leoni, O., Oria, C., Papagni, M., Nosetti, G., Caldiroli, E., Moser, V., Roni, R., Polverino, A., Bovo, C., Mezzalira, L., Andretta, M., Trentin, L., Palcic, S., Pettinelli, A., Arbo, A., Bertola, A., Capparoni, G., Cattaruzzi, C., Marcuzzo, L., Rosa, F. V., Basso, B., Saglietto, M., Delucis, S., Prioli, M.,

Filippi, R., Coccini, A., Ghia, M., Sanfelici, F., Radici, S., Scanavacca, P., Campi, A., Bianchi, S., Verzola, A., Morini, M., Borsari, M., Danielli, A., Dal Maso, M., Marsiglia, B., Vujovic, B., Pisani, M., Bonini, P., Lena, F., Aletti, P., Marcobelli, A., Sagratella, S., Fratini, S., Bartolini, F., Riccioni, G., Meneghini, A., Di Turi, R., Fano, V., Blasi, A., Pagnozzi, E., Quintavalle, G., D'Avenia, P., De Matthaeis, M.C., Ferrante, F., Crescenzi, S., Marziale, L., Venditti, P., Bianchi, C., Senesi, I., Baci, R., De Carlo, I., Lavalle, A., Trofa, G., Marcello, G., Pagliaro, C., Troncone, C., Farina, G., Tari, M.G., Motola, G., De Luca, F., Saltarelli, M.L., Granieri, C., Vulnera, M., Palumbo, L., La Viola, F., Florio, L., De Francesco, A.E., Costantino, D., Rapisarda, F., Lazzaro, P.L., Pastorello, M., Parlli, M., Visconti, M., Uomo, I., Sanna, P., Lombardo, F., 2015. Risk of hospitalization for heart failure in patients with type 2 diabetes newly treated with DPP-4 inhibitors or other oral glucose-lowering medications: a retrospective registry study on 127,555 patients from the Nationwide OsMed Health-DB Database. Eur. Heart J.

Larsen, J.J., Dela, F., Madsbad, S., Vibe-Petersen, J., Galbo, H., 1999. Interaction of sulfonylureas and exercise on glucose homeostasis in type 2 diabetic patients. Diabetes Care 22, 1647–1654.

Morgan, C.L., Mukherjee, J., Jenkins-Jones, S., Holden, S.E., Currie, C.J., 2014. Association between first-line monotherapy with sulphonylurea versus metformin and risk of all-cause mortality and cardiovascular events: a retrospective, observational study. Diabetes. Obes. Metab. 16, 957–962.

Mori, H., Chujo, M., Tanaka, E., Yamakawa, A., Shinozaki, Y., Mohamed, M.U., Nakazawa, H., 1995. Modulation of adrenergic coronary vasoconstriction via ATP-sensitive potassium channel. Am. J. Physiol. 268, H1077–H1085.

Nelson, M.T., Huang, Y., Brayden, J.E., Hescheler, J., Standen, N.B., 1990. Arterial dilations in response to calcitonin gene-related peptide involve activation of K+ channels. Nature 344, 770–773.

Noma, 1983. ATP-regulated K+ channels in cardiac muscle. Nature.

Qaseem, A., Humphrey, L.L., Sweet, D.E., Starkey, M., Shekelle, P., 2012. Oral pharmacologic treatment of type 2 diabetes mellitus: a clinical practice guideline from the American College of Physicians. Ann. Intern. Med. 156, 218–231.

Quast, U., Guillon, J.M., Cavero, I., 1994. Cellular pharmacology of potassium channel openers in vascular smooth muscle. Cardiovasc. Res. 28, 805–810.

Simpson, S.H., Majumdar, S.R., Tsuyuki, R.T., Eurich, D.T., Johnson, J.A., 2006. Dose-response relation between sulfonylurea drugs and mortality in type 2 diabetes mellitus: a population-based cohort study. CMAJ 174, 169–174.

Thomas, G.D., Hansen, J., Victor, R.G., 1997. Atp-sensitive potassium channels mediate contraction- induced attenuation of sympathetic vasoconstriction in rat skeletal muscle. J Clin Invest 99, 2602–2609.

Chapter 2 - Acute blockade of ATP-sensitive K^+ channels impairs skeletal muscle vascular control in rats during treadmill exercise

Abstract

The ATP-sensitive K^+ (K_{ATP}) channel is a class of inward rectifier K^+ channels that can link local O_2 availability to vasomotor tone across exercise-induced metabolic transients. This investigation tested the hypothesis that, if K_{ATP} channels are crucial to exercise hyperemia, inhibition via glibenclamide (GLI) would lower hindlimb skeletal muscle blood flow (BF) and vascular conductance (VC) during treadmill exercise. In 27 adult male Sprague Dawley rats mean arterial pressure (MAP), blood [lactate], and hindlimb muscle BF (radiolabelled microspheres) were determined at rest (n = 6) or during exercise (n = 6-8; 20, 40 and 60 m min^{-1}, 5% incline, i.e. ~60-100% maximal oxygen uptake) under control (CON) and GLI conditions (5 mg kg^{-1}, i.a). At rest and during exercise, MAP was higher (Rest: 17 ± 3, 20: 5 ± 1, 40: 5 ± 2, 60: 5 ± 1 %, $p < 0.05$) with GLI. Hindlimb muscle BF (16 ± 7, 30 ± 9, 20 ± 8 %) and VC (20 ± 7, 33 ± 8, 24 ± 8 %) were lower with GLI during exercise at 20, 40 and 60 m min^{-1} respectively ($p < 0.05$ for all), but not at rest. Within locomotory muscles there was a greater fractional reduction present in muscles comprised predominantly of type I and type IIa fibers at all exercise speeds ($p < 0.05$). Additionally, blood [lactate] was 106 ± 29 and 44 ± 15 % higher during exercise with GLI at 20 and 40 m min^{-1}, respectively ($p < 0.05$). That K_{ATP} channel inhibition reduces hindlimb muscle BF during exercise in rats supports the obligatory contribution of K_{ATP} channels in large muscle mass exercise-induced hyperemia.

Introduction

The appropriate redistribution of cardiac output at exercise onset is achieved by vascular smooth muscle cell (SMC) relaxation in arterioles supplying active skeletal muscle and SMC contraction in arterioles supplying quiescent tissue. Within the active skeletal muscle vascular bed, local metabolic byproducts of muscle contraction (e.g. ATP, H^+, K^+, adenosine, etc.) as well as endothelium derived factors (e.g. NO, PGI_2) are important for matching O_2 supply with O_2 demand during exercise (Dinenno and Joyner, 2004; Hellsten et al., 2012; Symons et al. 1999) via modulation of vascular tone. The SMC resting membrane potential supports this balance by setting vascular tone as well as determining vasomotor sensitivity to depolarizing stimuli (i.e. sympathetic nerve activity; SNA). Modulation of membrane potential may therefore represent an important mechanism by which sympathetic vasoconstriction is attenuated in active skeletal muscle (Thomas et al. 1997).

It is well recognized that the inward rectifier K^+ channels (Kir) influence membrane potential and are capable of hyperpolarizing the SMC membrane resulting in an inhibitory effect on excitability and thus relaxation (Nelson and Quayle, 1995). Specifically, the vascular ATP-sensitive K^+ (K_{ATP}) channel is activated, in part, by the accumulation of subsarcolemmal ADP and may therefore contribute to the integration of local O_2 availability with vasomotor control across the greater than 2 orders of magnitude increase in muscle metabolism seen with exercise. Importantly, K_{ATP} channel activation has been shown to result in SMC hyperpolarization, relaxation of vascular smooth muscle and attenuated α-adrenergic vasoconstriction (Mori et al., 1995; Nakai and Ichihara, 1994; Quast et al., 1994; Tateishi and Faber, 1995). In healthy human forearm muscle the activation of K_{ATP} channels increases vasodilation in response to ischemia indicating the potential for K_{ATP} channels to contribute substantially to skeletal muscle O_2

delivery during exercise (Bijlstra et al., 1996b). Despite early studies demonstrating that blockade of K_{ATP} channels significantly attenuates reactive and functional hyperemia in humans and animals (Bank et al., 2000; Banitt et al., 1996; Bijlstra et al. 1996a) more recent work has failed to confirm these results (Duncker et al., 2001; Farouque and Meredith, 2003; Schrage et al., 2006). As vasomotor control mechanisms may be fiber type dependent (e.g. Behnke et al., 2011; Copp et al., 2010; Hirai et al., 1994) it is quite possible that, within muscles with specific-fiber type composition, K_{ATP} channel activation may represent an obligatory mechanism supporting exercise-induced skeletal muscle hyperemia *in vivo*. Additionally, given that K_{ATP} channels are sensitive to metabolic status and that there exists considerable heterogeneity of metabolic characteristics among and within skeletal muscles it is plausible that K_{ATP} channel-mediated vasodilation is dependent upon skeletal muscle fiber type distribution; a concept that cannot be addressed in humans with current technology. The differences in fiber type profile between species, muscles or states of dysfunction promotes remarkably different muscle O_2 tensions which may determine ADP accumulation and the open probability of K_{ATP} channels in the skeletal muscle vasculature.

The purpose of the present investigation was to test the hypothesis that inhibition of K_{ATP} channels via glibenclamide (GLI) would reduce hindlimb skeletal muscle blood flow (BF) and vascular conductance (VC) and increase arterial blood [lactate] during submaximal treadmill exercise in healthy rats. Furthermore, given the purported coupling of cellular metabolism with vasomotor tone by K_{ATP} channels, it was anticipated that the reductions in VC with GLI would associate directly with the percentage of type I and type IIa fibers across muscles.

Methods

Ethical approval

All procedures were approved by the Institutional Animal Care and Use Committee of Kansas State University under the guidelines established by the National Institutes of Health and conducted according to the animal use guidelines mandated by *The Journal of Physiology* (Drummond, 2009). 27 adult male Sprague-Dawley rats (~4 months old, body mass = 366 ± 7 g) were maintained in accredited animal facilities (Association for the Assessment and Accreditation of Laboratory Animal Care) at Kansas State University on a 12-h light/12-h dark cycle with food and water provided *ad libitum*. Rats were separated into either rest (n = 6) or 3 exercise (n = 6-8) groups and used for within-animal comparisons under control (CON) and K_{ATP} channel inhibition (GLI) conditions. Rats were acclimatized to running during a familiarization period comprised of 5-7 sessions on a custom-built motor-driven treadmill set at an incline of 5%. Each session consisted of running at progressive speeds from ~20 m min^{-1} to ~60 m min^{-1} over a total duration of no more than 5 min.

The pharmacological sulphonylurea derivative GLI (494 g mol^{-1}; 5-chloro-*N*-(4-[*N*-(cyclohexylcarbamoyl)sulfamoyl]phenethyl)-2-methoxybenzamide; Sigma-Aldrich, St Louis, MO, USA) was used to achieve inhibition of vascular K_{ATP} channels. Briefly, 50 mg of GLI was dissolved in 4 ml of NaOH (0.1 M) under continuous sonication to produce a 12.5 mg ml^{-1} stock solution. A 5 mg kg^{-1} dose was drawn from the stock solution and diluted to ~1 ml with heparinized saline. Thomas et al. demonstrated that 20 mg/kg i.v. of glibenclamide reverses the effect of the same dose of diazoxide (Thomas et al., 1997). However, it has been reported previously that GLI is a selective K_{ATP} channel blocker at concentrations below 5 μmol L^{-1} (Beech et al., 1993; Sadraei and Beech, 1995). The current dose of 5 mg kg^{-1} for rats of a mean

body mass of 366 g equates to a blood concentration of ~140 μmol L^{-1}. Given that 98-99% of GLI is bound to plasma protein, the effective blood concentration of GLI is ~2-3 μmol L^{-1} (George et al., 1990) which is in the range for GLI to be selective for K_{ATP} channels without possible inhibition of Ca^{+} channel current (Sadraei and Beech, 1995). This dosing strategy, based on smooth muscle cell investigations was shown to elicit a degree of K_{ATP} channel blockade for swine *in vivo* (60-70%; Duncker et al., 2001).

Surgical instrumentation

On the day of the final protocol the rats were anesthetized initially with a 5% isoflurane-O_2 mixture and maintained on a 3% isoflurane-O_2 mixture for the duration of the surgical instrumentation. Cannulation of both the carotid and caudal arteries was performed with PE-10 connected to PE-50 (Intra-Medic polyethylene tubing, BD, Franklin Lakes, NJ, USA). The catheters were then tunneled subcutaneously to the dorsal aspect of the cervical region where they were exteriorized through a puncture wound in the skin. Following closure of incisions the rat was removed from anesthesia and given a minimum recovery period of 2 h.

Experimental protocol

After the recovery period the exercise BF protocol was performed with the treadmill set at an incline of 5%. The rat was placed on the treadmill and the carotid catheter was attached to a pressure transducer (P23ID, Gould Statham Instruments, Hato Rey, Puerto Rico, USA) for the measurement of mean arterial pressure (MAP) and heart rate (HR) while the caudal catheter was connected to a 1-ml syringe attached to a Harvard pump (model 907, Holliston, MA, USA). Exercise (i.e. ~60-100% maximal oxygen uptake, $\dot{V}O_2max$) was initiated at a speed of 20 (n = 8), 40 (n = 6) or 60 m min^{-1} (n = 7) and remained steady for ~3 min at which time pre-microspheres HR and pressures were recorded. At ~3.5 min of total exercise time blood withdrawal was

initiated from the caudal catheter at a rate of 0.25 ml min^{-1}. The carotid catheter was then disconnected from the pressure transducer and ~0.5-0.6 10^6, 15 μm diameter microspheres (^{57}Co or ^{85}Sr in random order, Perkin Elmer Life and Analytical Sciences, Waltham, MA, USA) were rapidly infused into the aortic arch of the running animal for the determination of tissue BF. Upon reconnection of the carotid catheter to the pressure transducer a second pressure reading was immediately recorded post-microspheres. An arterial blood sample (0.2 ml) was then drawn from the carotid artery catheter for the determination of blood gases, hematocrit, pH, [lactate] and [glucose]. Exercise was terminated and the rat was continuously monitored during a minimum 30 min rest period before the second bout began.

A post-recovery pressure was recorded to establish resting pressure and HR values. The K_{ATP} channel inhibitor GLI (5 mg kg^{-1}) was infused via the caudal artery catheter. Pressure was monitored continuously until GLI elicited a persistent rise in MAP at which time the second exercise bout was initiated. The second bout and administration of microspheres were performed identically to the protocol described above. As demonstrated previously, subsequent control bouts of exercise for this protocol demonstrate high reproducibility of hemodynamic variables (MAP, HR, BF and VC; Sadraei and Beech, 1995). Upon exercise termination the rat was euthanized with an overdose of pentobarbital (>50 mg kg^{-1} body mass) via the carotid artery catheter. For another group of rats (n = 6) administration of microspheres, blood sampling and pressure recordings were performed at rest under CON and GLI conditions as described above.

Determination of BF and VC

Correct placement of the carotid catheter in the aortic arch was verified by anatomical dissection. Hindlimb muscles and muscle portions as well as the lungs, kidneys, and

representative organs of the splanchnic region were removed, weighed and placed in counting vials for the determination of radioactivity.

Radioactivity was measured for each tissue as well as the reference sample using a gamma scintillation counter (model 5230, Packard Auto Gamma Spectrometer, Downers Grove, IL, USA). Taking into account the cross-talk fraction between isotopes enabled radioactivity to be determined for separate microsphere injections (^{57}Co or ^{85}Sr). Based on this radioactivity BF to each tissue was determined for the individual conditions, CON or GLI, by comparison to the reference sample of known flow rate and measured radioactivity (Ishise et al., 1980; Musch and Terrell, 1992). Tissue BFs were expressed as ml min^{-1} (100 g)$^{-1}$ of tissue and the results were also normalized to MAP and expressed as VC (ml min^{-1} (100 g)$^{-1}$ mmHg^{-1}). Adequate mixing of the microspheres for each BF determination was verified by a <15% difference in BF between the right and left kidneys or right and left hindlimbs.

Statistical analysis

All variables were compared between and within groups using mixed two-way ANOVA's and Student-Newman-Keuls *post hoc* tests where appropriate. Muscle fiber type composition was based on the percentage of type I, type IIa, type IIb, and type IId/x fibers in the individual muscles and muscle parts of the rat hindlimb as reported by Delp and Duan (1996). Pearson Product Correlations were used to test the relationship between changes in VC and muscle fiber type. Significance was set at $p < 0.05$ and values are expressed as mean ± SEM.

Results

There was no significant difference in body mass between groups (Rest: 365 ± 5, 20: 367 ± 13, 40: 407 ± 26, 60: 375 ± 15 g, $p > 0.05$).

Effects of GLI on HR, MAP, arterial blood gases, pH, hematocrit, [lactate] and [glucose]

At rest and during exercise at all speeds MAP was higher with GLI compared to CON (Fig. 1). HR was lower with GLI only at rest and during exercise at 20 m min^{-1}. Administration of the vehicle did not change MAP (Pre-vehicle: 127 ± 4, Post-vehicle: 125 ± 4 mmHg, $p > 0.05$) or HR (Pre-vehicle: 400 ± 18, Post-vehicle: 436 ± 19 mmHg, $p > 0.05$) in a subset of rats ($n = 6$). Arterial PO_2 was higher with GLI at rest (CON: 96.8 ± 2.2 GLI: 107.7 ± 2.6 mmHg, $p < 0.05$) but not during exercise at any speed ($p > 0.05$ for all). Hematocrit was higher with GLI during exercise at 20 m min^{-1} only (CON: 31 ± 1, GLI: 33 ± 1 %, $p < 0.05$) while pH was lower with GLI during exercise at 40 m min^{-1} only (CON: 7.39 ± 0.02, GLI: 7.35 ± 0.03, $p < 0.05$). During exercise at both 40 (CON: 102 ± 6, GLI: 89 ± 8 mg dL^{-1}) and 60 m min^{-1} (CON: 87 ± 4, GLI: 75 ± 3 mg dL^{-1}) blood [glucose] was lower with GLI ($p < 0.05$ for both). Blood [lactate] was higher with GLI during exercise at 20 (CON: 2.0 ± 0.3, GLI: 4.1 ± 0.9 mmol L^{-1}, $p < 0.05$) and 40 m min^{-1} (CON: 5.9 ± 0.5, GLI: 8.7 ± 1.4 mmol L^{-1}, $p < 0.05$) but not at rest or 60 m min^{-1} ($p > 0.05$ for both).

Effects of GLI on skeletal muscle BF and VC

At rest there were no differences between groups in total hindlimb skeletal muscle BF or VC (Fig. 2, $p = 0.40$) or BF and VC to any of the individual muscles or muscle portions (Table 1). During exercise at all speeds both total hindlimb skeletal muscle BF and VC were lower with GLI compared to CON (Fig. 2). Specifically, GLI resulted in a lower BF in 13, 20, and 14 of the

28 individual hindlimb muscles or muscle portions during exercise at 20, 40 and 60 m min^{-1}, respectively (Table 2). VC was lower with GLI in 15, 21, and 18 of the 28 individual hindlimb muscles or muscle portions during exercise at 20, 40 and 60 m min^{-1}, respectively (Table 3). Furthermore, there was a significant positive correlation between the percentage of type I and type IIa fibers and the percent decrease in VC for the 28 muscles or muscle portions of the hindlimb during exercise at 20 ($r = -0.53$), 40 ($r = -0.69$) and 60 m min^{-1} ($r = -0.50$).

Effects of GLI on renal and splanchnic BF and VC at rest and during exercise

Renal BF and VC were reduced by GLI at rest but not during exercise at any speed (Table 3). Among the representative organs of the splanchnic region BF was reduced at rest to the spleen, adrenals and large intestine with GLI. VC was reduced at rest to the stomach, adrenals, spleen, pancreas, small intestine and large intestine with GLI. BF during exercise at 20 m min^{-1} was reduced with GLI to the pancreas and small intestine, and VC was reduced to the stomach, pancreas and small intestine (Table 3). There was no difference in BF or VC between CON and GLI for any organs at 40 or 60 m min^{-1}. However, at 40 and 60 m min^{-1} the CON renal, adrenal, pancreas and small intestine BF's were lower compared to 20 m min^{-1}. Similarly, renal, stomach, pancreas and large intestine VC's were lower at both 40 and 60 compared to 20 m min^{-1}.

Discussion

The primary original findings of this investigation were that the inhibition of K_{ATP} channels in the rat via GLI during exercise increased MAP and decreased HR, reduced hindlimb skeletal muscle BF and VC and increased blood [lactate]. Furthermore, the decrease in VC with GLI reflected a fiber type-selective effect such that VC was reduced primarily to the muscles comprised of type I and type IIa fibers. The strength of the fiber type relationship persisted at higher speeds where muscle recruitment increasingly represents the complete spectrum of fiber types. These data support that K_{ATP} channels contribute significantly to exercise-induced skeletal muscle hyperemia during treadmill exercise in rats.

The finding that GLI increased MAP at rest with a consequent decrease in HR is not surprising as this is consistent with previous reports at rest in conscious rats (Gardiner et al., 1996; Moreau et al., 1994), swine (Duncker et al., 2001) and humans (Farouque and Meredith, 2003). Specifically, the higher MAP and lower HR at rest with K_{ATP} channel inhibition were coincident with large reductions in renal and splanchnic VC and suggest the occurrence of K_{ATP} channel inhibition. This is in agreement with studies demonstrating a significant contribution of K_{ATP} channels to basal vasomotor tone in the systemic circulation of conscious rats (Gardiner et al., 1996, Moreau et al., 1994; Parekh and Zou, 1996), hamsters (Jackson, 1993; Saito et al., 1996) and dogs (Comtois et al., 1994; Vanelli and Hussain, 1994).

The similar hindlimb skeletal muscle BF and VC at rest with GLI is most likely due to the inhibition of K_{ATP} channels at physiological ATP concentrations or a compensatory vasodilation by redundant pathways (e.g. NO, PGI_2, baroreflex) to maintain appropriate basal vasomotor tone (Hellsten et al., 2012). Similar observations have been made across species

(Duncker et al, 2001; Farouque and Meredith, 2003) although there is some evidence for modest skeletal muscle vascular K_{ATP} channel activity at rest (Nielsen et al., 2003).

Previously, K_{ATP} channel blockade in rats and hamsters has been shown to reduce the skeletal muscle hyperemic response to electrically-induced contractions (Saito et al, 1996; Thomas et al., 1997). In this regard, our findings indicate that, in rats, K_{ATP} channel inhibition also reduces the *in vivo* skeletal muscle hyperemic response to treadmill running. This corroborates the notion that K_{ATP} channels represent an important mechanistic link between metabolism and vasomotor tone during exercise. The 20% decrease in hindlimb skeletal muscle VC during exercise at 20 m min^{-1} with GLI suggests that the rat locomotor muscle vascular bed contains a substantial pool of K_{ATP} channels which are activated even at moderate exercise intensities. Importantly, the 16% decrease in exercising hindlimb skeletal muscle BF occurred simultaneous with a doubling of arterial blood [lactate] (2.0 to 4.1 mmol L^{-1}) with GLI at 20 and a 44% increase at 40 m min^{-1}; an effect not seen at rest. Thus, not only is vasodilation attenuated in the hindlimb vasculature, but this decrement represents an impaired vasomotor control failing to meet the BF demands of the active skeletal muscle. These intriguing findings support the hypothesis that K_{ATP} channels are obligatory for exercise-induced hyperemia with respect to exercise tolerance and work capacity; at least within the rat. Furthermore, the magnitude of the K_{ATP} channel role may actually be underestimated herein. We acknowledge that incomplete K_{ATP} channel blockade may be present given that the precise degree of inhibition was not established. Consequently, the data herein may reflect only a portion of the K_{ATP} channel contribution to exercise-induced hyperemia. Regardless, the results demonstrate clearly the significant effects of GLI on skeletal muscle BF, VC and arterial blood [lactate]. The substantial increase of arterial blood [lactate] at 20 and 40 m min^{-1} is not surprising given that GLI-induced decreases in BF

were correlated with the percent type I and IIa fibers such that the predominantly oxidative muscles and muscle portions experienced the most consistent decrease in BF during exercise. The muscle fiber type composition explains ~28, 48 and 25% of the VC decrease with GLI at 20, 40 and 60 m min^{-1}, respectively. The preferential recruitment of type I and type IIa fibers during the low speed exercise protocol (~55-65% $\dot{V}O_{2max}$) is likely to account for a substantial portion of the fiber type-selective effect at 20 m min^{-1}. However, the relationship persisted even at 40 and 60 m min^{-1} when a greater proportion of type IIb/dx fibers were recruited. NO, which has a proportionally greater role in the control of oxidative fiber type vascular beds (Hirai et al., 1994), has been shown to operate through the activation of K_{ATP} channels (Murphy and Brayden, 1995; Tare et al., 1990). Thus, inhibition of K_{ATP} channels in the vasculature supplying type I and IIa fibers would result in a greater decrement of VC during exercise as it may block a portion of this NO-mediated vasodilation. Investigating the sensitivity of the fiber type relationship to work rates above and below fundamental physiological tipping points such as critical speed/power, lactate threshold, etc. may prove insightful.

With respect to the interpretation of the effects of GLI on altered BF and VC as purely local muscle effects, the possible impacts of K_{ATP} channel inhibition on sympathetic nerve discharge must be considered. The loss of K_{ATP} channel-mediated hyperpolarization could conceivably result in increased sympathetic nerve discharge for a given stimulus which would account, in part, for the decrements in BF and VC seen herein. However, we consider this unlikely because it has been demonstrated, in male Sprague Dawley rats, that direct injection of GLI into the rostral ventrolateral medulla has no effect on blood pressure, HR or renal SNA (Guo et al., 2011). These findings support that GLI did not directly impact sympathetic nerve

discharge in the current study and that the reductions in BF and VC are the result, specifically, of muscle vascular K_{ATP} channel inhibition.

It is important to note that the BF and VC results seen herein run contrary to data from exercising swine (Duncker et al., 2001). This may be the result of cross-species differences in vascular K_{ATP} channel expression and/or function. Indeed, while the octameric structure of vascular K_{ATP} channels is presumed to be the Kir6.1 pore-forming units with associated SUR2B subunits, considerable heterogeneity of functional expression has been demonstrated through readily occurring heteromultimerization of the pore forming units (Kir6.x) as well as the sulphonylurea receptor subunits (SURx) which confer the channel's ATP sensitivity. Accordingly, there is substantial variation in unitary conductance which may impact the relative importance of the K_{ATP} channel in vasomotor control across species, tissue beds, and metabolic rates (rev. by Teramoto, 2006). This is particularly true for vascular K_{ATP} channels as the range of unitary conductance appears to be much greater (~20 to >200 pS) than for pancreatic β cells (~50 to 90 pS) and some regions of the heart and brain (~40 to 80 pS) (Cole and Clément-Chomienne, 2003). Further exploration of the discrepancies in channel molecular structure across tissues may lead to better understanding of the functional consequences resulting from global K_{ATP} channel blockade.

The role of K_{ATP} channels in the control of human skeletal muscle BF has been elucidated primarily by the use of K_{ATP} channel agonists, namely nicorandil and diazoxide, as well as the K_{ATP} channel inhibitor GLI. Seminal results include K_{ATP} channel agonists eliciting forearm vasodilation (Bijlstra et al., 1996a) and K_{ATP} channel blockade reducing the BF response to both reactive and functional hyperemia in some (Bank et al., 2000; Banitt et al., 1996; Bijlstra et al., 1996b) but not all studies (Duncker et al., 2001, Schrage et al., 2006). The reason for the

differential conclusions drawn from use of K_{ATP} channel agonists versus blockers is unclear. In healthy humans, K_{ATP} channels may not be obligatory for achieving adequate skeletal muscle BF during exercise given the great redundancy of vasodilatory mediators (Hellsten et al., 2012). The potential for parallel pathways such as NO- and PGI_2-mediated vasodilation to adequately meet BF requirements is present at relatively low workloads. This notion is consistent with K_{ATP} blockade studies in humans involving the forearm musculature which represents a small, non-locomotory portion of the total body muscle mass. Furthermore, the putative variability of K_{ATP} channel expression among skeletal muscle vascular beds with vastly different metabolic characteristics may confound interpretation of the available human data. It appears that the vascular K_{ATP} channel subtype uniquely requires nucleotide diphosphates (i.e. ADP) for activation and thus is designated as a nucleotide-dependent K^+ channel (K_{NDP}; Beech et al., 1993). As such, the channel would only demonstrate obligatory function where sufficiently low local muscle O_2 tension results in pronounced vascular subsarcolemmal ADP accumulation. Under these conditions even a small impact of K_{ATP} channel activation on SMC membrane potential could drive large increases in vasodilation. This is due to the remarkably steep relationship between membrane potential and Ca^{2+} influx in smooth muscle; changes of only a couple of millivolts can reduce $[Ca^{2+}]_i$ ~30% (Nelson et al., 1990). For this reason, we are in agreement with Shrage et al (2006) who have recognized that the determination of K_{ATP} channel function across more diverse muscle vascular beds and a greater range of exercise intensities/paradigms is necessary to resolve the circumstances under which these channels impact O_2 delivery. The *in vivo* measurements evaluating 28 muscles and muscle portions seen herein demonstrates the novel information to be gained from this approach.

The results seen herein suggest that the role of K_{ATP} channels may be potentiated under conditions of low local muscle O_2 tension (i.e. when muscle fibers are recruited) which can increase vascular glycolytic flux and drive greater intracellular ADP accumulation. This environment is exacerbated in muscle fibers exposed to high metabolic demand as well as conditions characterized by skeletal muscle hypoxia such as heart failure (rev. by Poole et al., 2012) type II diabetes (Cunha et al., 2008; Padilla et al., 2007) and aging (Poole and Ferreira, 2007). Therefore, the potential for K_{ATP} channels to contribute significantly to exercise-induced skeletal muscle hyperemia has important implications for characterizing the etiology of blood-muscle O_2 transport decrements in these conditions.

Experimental considerations

A major strength of the current experimental design is that each animal acts as its own control for the effects of GLI thus increasing statistical power and reducing animal use. However, the limitation of only 2 available isotopes precludes BF controls for the vehicle being performed in the same animal. To minimize animal use per IUCAC mandate, the effect of the vehicle on MAP and HR was assessed in a subset of animals (n = 6) with no change evident after administration of the vehicle. Furthermore, a similar NaOH/saline vehicle was shown to have no impact on the vascular hemodynamic response to contractions in Sprague Dawley rats (Thomas et al., 1997).

Since GLI is not selective for vascular smooth muscle K_{ATP} channels it might be argued that GLI-induced K_{ATP} channel inhibition in the coronary vasculature or cardiac myocytes could account for the reduced BF during exercise seen herein. Measurements of coronary BF and VC were not available in the present investigation. However, decrements in cardiac output would not be expected to support a decrease in BF for select muscles or muscle portions as seen herein.

Likewise, the increase in MAP with GLI would not be consistent with decrements in cardiac output. These observations suggest that GLI does not impact coronary BF such that decrements in cardiac function (and reduced cardiac output) underlie the decrease in hindlimb skeletal muscle BF during submaximal treadmill exercise found herein. Additionally, given that inhibition of endothelial K_{ATP} channels can be achieved via GLI, the effects of K_{ATP} channel inhibition on vascular control may be mediated via altered endothelial function rather than a direct action on SMCs (Malester et al., 2007). However, the conclusion that K_{ATP} channels contribute to skeletal muscle vascular control during large muscle mass exercise in rats is independent of the ability to partition endothelial influence from direct SMC effects.

The existence of mitochondrial membrane K_{ATP} channels requires the consideration that altered muscle O_2 consumption or extraction impacts skeletal muscle BF. The limited evidence available for whole body exercising $\dot{V}O_2$ indicates no change with GLI (Larsen et al., 1999). This might be expected given that mitochondrial K_{ATP} channel blockade does not appear to alter the O_2 cost of exercise per se. Furthermore, if an increase in O_2 consumption occurred during treadmill exercise with GLI the regulation of O_2 supply-demand described previously would dictate an increase in hindlimb skeletal muscle BF with GLI rather than the decrease seen herein. While O_2 extraction for a given $\dot{V}O_2$ can increase with K_{ATP} channel blockade in cardiac muscle during submaximal exercise (Duncker et al., 2001) this effect, as dictated by the Fick equation, serves to offset the GLI-induced reductions in BF. Crucially, the use of mitochondrial-selective K_{ATP} channel blockers verifies that the GLI-induced reduction of myocardial $\dot{V}O_2$ in the canine during exercise is the result of reduced myocardial BF rather than a primary mitochondrial respiration effect (Chen et al., 2001). Thus, changes in O_2 extraction or consumption appear to be

driven by impaired vascular control rather than a direct result of mitochondrial K_{ATP} channel inhibition.

Conclusions

Our principal novel findings show that inhibition of K_{ATP} channels via GLI (5 mg kg^{-1}) attenuates hindlimb skeletal muscle BF and VC and elevates blood [lactate] during submaximal treadmill exercise. The effects of K_{ATP} channel inhibition were significant across the range of exercise speeds employed and demonstrated a fiber type-selectivity within muscles comprised of highly oxidative fibers. These results provide compelling evidence that K_{ATP} channel-induced hyperpolarization constitutes an important mechanism of vasomotor control in exercising skeletal muscle supporting that K_{ATP} channels represent an obligatory pathway for skeletal muscle vascular control during large muscle mass exercise in healthy rats.

Table 2-1. Effects of GLI on individual hindlimb skeletal muscle BFs (ml min^{-1} $(100\ g)^{-1}$) and VCs (ml min^{-1} $(100\ g)^{-1}$ $mmHg^{-1}$) for the rest group

	BF		VC	
	CON	GLI	CON	GLI
Ankle extensors				
Soleus (91%)	115 ± 20	91 ± 28	0.88 ± 0.15	0.62 ± 0.21
Plantaris (20%)	18 ± 4	16 ± 4	0.14 ± 0.03	0.11 ± 0.03
Gastrocnemius, red (86%)	57 ± 18	46 ± 22	0.44 ± 0.15	0.30 ± 0.14
Gastrocnemius, white (0%)	11 ± 3	16 ± 5	0.09 ± 0.03	0.10 ± 0.03
Gastrocnemius, mixed (9%)	20 ± 5	20 ± 9	0.16 ± 0.04	0.13 ± 0.06
Tibialis posterior (27%)	26 ± 10	11 ± 4	0.21 ± 0.08	0.07 ± 0.02
Flexor digitorum longus (32%)	57 ± 31	65 ± 48	0.41 ± 0.21	0.38 ± 0.26
Flexor halicus longus (29%)	16 ± 4	9 ± 2	0.12 ± 0.03	0.06 ± 0.01
Ankle flexors				
Tibialis anterior, red (37%)	59 ± 17	33 ± 12	0.45 ± 0.13	0.20 ± 0.06
Tibialis anterior, white (20%)	24 ± 8	17 ± 4	0.19 ± 0.06	0.11 ± 0.03
Extensor digitorum longus (24%)	22 ± 5	20 ± 5	0.16 ± 0.04	0.13 ± 0.03
Peroneals (33%)	27 ± 7	18 ± 7	0.22 ± 0.06	0.12 ± 0.04
Knee extensors				
Vastus intermedius (96%)	134 ± 34	101 ± 44	1.04 ± 0.28	0.70 ± 0.30
Vastus medialis (18%)	38 ± 14	30 ± 12	0.30 ± 0.12	0.20 ± 0.08
Vastus lateralis, red (65%)	88 ± 37	87 ± 45	0.71 ± 0.31	0.59 ± 0.29
Vastus lateralis, white (0%)	10 ± 2	14 ± 4	0.08 ± 0.01	0.10 ± 0.03
Vastus lateralis, mixed (11%)	24 ± 8	24 ± 8	0.19 ± 0.07	0.16 ± 0.05
Rectus femoris, red (34%)	38 ± 11	28 ± 13	0.29 ± 0.08	0.18 ± 0.09
Rectus femoris, white (0%)	21 ± 4	16 ± 5	0.17 ± 0.04	0.11 ± 0.03
Knee flexors				
Biceps femoris anterior (0%)	12 ± 3	12 ± 2	0.10 ± 0.03	0.08 ± 0.02
Biceps femoris posterior (8%)	20 ± 7	16 ± 5	0.16 ± 0.05	0.10 ± 0.03
Semitendinosus (17%)	23 ± 7	15 ± 4	0.19 ± 0.06	0.10 ± 0.02
Semimembranosus, red (28%)	25 ± 12	17 ± 4	0.20 ± 0.09	0.12 ± 0.03
Semimembranosus, white (0%)	13 ± 2	10 ± 1	0.10 ± 0.02	0.07 ± 0.01
Thigh adductors				
Adductor longus (95%)	97 ± 14	74 ± 20	0.76 ± 0.11	0.50 ± 0.15
Adductor magnus & brevis (11%)	31 ± 14	22 ± 7	0.25 ± 0.11	0.15 ± 0.05
Gracilis (23%)	23 ± 9	14 ± 3	0.18 ± 0.07	0.09 ± 0.02
Pectineus (31%)	29 ± 10	20 ± 6	0.23 ± 0.08	0.13 ± 0.04

Data are mean ± SEM. Values in parentheses indicate % type I + IIa according to Delp & Duan (1996). Rest; $n = 6$, Exercise; $n = 8$. *$P < 0.05$ *versus* control.

Table 2-2. Effects of GLI on individual hindlimb skeletal muscle BFs for exercise groups

	20		40		60	
	CON	GLI	CON	GLI	CON	GLI
Ankle extensors						
Soleus (91%)	382 ± 19	277 ± 21*	293 ± 63	152 ± 25*†	312 ± 15	213 ± 28*
Plantaris (20%)	253 ± 25	209 ± 21	254 ± 35	193 ± 32*	258 ± 15	223 ± 10
Gastrocnemius, red (86%)	419 ± 40	337 ± 33*	395 ± 70	238 ± 52*	432 ± 11	351 ± 41
Gastrocnemius, white (0%)	53 ± 13	69 ± 9	82 ± 15	81 ± 11	93 ± 13	85 ± 11
Gastrocnemius, mixed (9%)	161 ± 9	152 ± 16	182 ± 28	137 ± 21*	201 ± 9	167 ± 13*
Tibialis posterior (27%)	192 ± 23	161 ± 16	229 ± 37	162 ± 20*	285 ± 22	222 ± 21*
Flexor digitorum longus (32%)	118 ± 17	105 ± 20	116 ± 8	86 ± 16	122 ± 11	124 ± 15
Flexor halicus longus (29%)	107 ± 14	87 ± 12*	117 ± 21	84 ± 15*	107 ± 12	96 ± 10
Ankle flexors						
Tibialis anterior, red (37%)	383 ± 24	337 ± 39	420 ± 63	270 ± 40*	405 ± 23	334 ± 40
Tibialis anterior, white (20%)	136 ± 12	139 ± 18	157 ± 24	93 ± 17*	127 ± 14	117 ± 15
Extensor digitorum longus (24%)	70 ± 5	72 ± 5	128 ± 27†	97 ± 15	94 ± 9	97 ± 13
Peroneals (33%)	169 ± 13	144 ± 19	172 ± 22	112 ± 9*	149 ± 17	122 ± 10
Knee extensors						
Vastus intermedius (96%)	419 ± 25	299 ± 18*	407 ± 69	262 ± 40*	456 ± 16	321 ± 31*
Vastus medialis (18%)	249 ± 15	186 ± 11*	245 ± 34	169 ± 27*	277 ± 15	221 ± 15*
Vastus lateralis, red (65%)	464 ± 27	306 ± 42*	325 ± 48†	196 ± 44*	396 ± 26	291 ± 36*
Vastus lateralis, white (0%)	56 ± 20†	57 ± 14	68 ± 12	68 ± 14	99 ± 7	82 ± 11
Vastus lateralis, mixed (11%)	200 ± 12†	139 ± 16*	186 ± 21	123 ± 25*	236 ± 20	180 ± 15*
Rectus femoris, red (34%)	324 ± 29	233 ± 25*	280 ± 33	196 ± 23*	333 ± 21	263 ± 26*
Rectus femoris, white (0%)	146 ± 15	113 ± 10*	141 ± 15	113 ± 18	187 ± 12‡	146 ± 13*
Knee flexors						
Biceps femoris anterior (0%)	34 ± 4	41 ± 6	72 ± 16†	62 ± 10	74 ± 5	63 ± 7
Biceps femoris posterior (8%)	106 ± 11	93 ± 10	119 ± 15	78 ± 17*	138 ± 11	103 ± 15*
Semitendinosus (17%)	77 ± 7	77 ± 15	73 ± 9	45 ± 4*	50 ± 9	50 ± 8
Semimembranosus, red (28%)	137 ± 19	123 ± 14	173 ± 16	110 ± 17*	215 ± 14	170 ± 20*‡
Semimembranosus, white (0%)	40 ± 6	47 ± 7	59 ± 10	41 ± 8*	91 ± 15‡	76 ± 15*‡
Thigh adductors						
Adductor longus (95%)	396 ± 18	251 ± 32*	254 ± 50†	111 ± 12*†	273 ± 31	164 ± 22*
Adductor magnus & brevis (11%)	142 ± 10	99 ± 6*	118 ± 6	86 ± 9*	147 ± 15	118 ± 13*
Gracilis (23%)	81 ± 13	58 ± 7*	69 ± 11	57 ± 12	66 ± 18	55 ± 11
Pectineus (31%)	104 ± 19	58 ± 8*	112 ± 19	83 ± 25	77 ± 14	55 ± 5

Data are mean ± SEM. Values in parentheses indicate % type I + IIa according to Delp & Duan (1996). Rest; $n = 6$, Exercise; $n = 8$. *$P < 0.05$ *versus* control

Table 2-3. Effects of GLI on individual hindlimb skeletal muscle VCs for exercise groups

	20		40		60	
	CON	GLI	CON	GLI	CON	GLI
Ankle extensors						
Soleus (91%)	2.76 ± 0.20	1.92 ± 0.20*	2.04 ± 0.48	0.99 ± 0.15*†	2.21 ± 0.11	1.44 ± 0.19*
Plantaris (20%)	1.83 ± 0.21	1.45 ± 0.18*	1.75 ± 0.26	1.26 ± 0.21*	1.84 ± 0.12	1.50 ± 0.07
Gastrocnemius, red (86%)	3.02 ± 0.32	2.33 ± 0.27*	2.75 ± 0.56	1.56 ± 0.34*	3.07 ± 0.14	2.38 ± 0.30*
Gastrocnemius, white (0%)	0.37 ± 0.08	0.47 ± 0.07	0.56 ± 0.11	0.53 ± 0.07	0.67 ± 0.11	0.58 ± 0.08
Gastrocnemius, mixed (9%)	1.15 ± 0.06	1.04 ± 0.13	1.26 ± 0.22	0.90 ± 0.14*	1.44 ± 0.10	1.14 ± 0.10*
Tibialis posterior (27%)	1.36 ± 0.14	1.10 ± 0.10	1.57 ± 0.25	1.06 ± 0.13*	2.01 ± 0.14‡	1.50 ± 0.14*
Flexor digitorum longus (32%)	0.84 ± 0.12	0.71 ± 0.13	0.80 ± 0.07	0.56 ± 0.10	0.88 ± 0.10	0.83 ± 0.09
Flexor halicus longus (29%)	0.75 ± 0.09	0.59 ± 0.09*	0.80 ± 0.14	0.54 ± 0.09*	0.77 ± 0.10	0.65 ± 0.07
Ankle flexors						
Tibialis anterior, red (37%)	2.76 ± 0.20	2.32 ± 0.28	2.92 ± 0.50	1.77 ± 0.26*	2.88 ± 0.17	2.24 ± 0.27*
Tibialis anterior, white (20%)	0.98 ± 0.09	0.96 ± 0.12	1.10 ± 0.19	0.61 ± 0.11*	0.90 ± 0.10	0.79 ± 0.10
Extensor digitorum longus (24%)	0.50 ± 0.04	0.49 ± 0.03	0.87 ± 0.17†	0.63 ± 0.09*	0.67 ± 0.08	0.65 ± 0.08
Peroneals (33%)	1.22 ± 0.10	0.99 ± 0.13*	1.19 ± 0.17	0.73 ± 0.06*	1.06 ± 0.12	0.82 ± 0.07*
Knee extensors						
Vastus intermedius (96%)	3.00 ± 0.18	2.06 ± 0.16*	2.79 ± 0.48	1.69 ± 0.24*	3.24 ± 0.15	2.15 ± 0.20*
Vastus medialis (18%)	1.79 ± 0.13	1.29 ± 0.11*	1.68 ± 0.24	1.10 ± 0.17*	1.97 ± 0.14	1.49 ± 0.10*
Vastus lateralis, red (65%)	3.34 ± 0.24	2.12 ± 0.34*	2.23 ± 0.34†	1.28 ± 0.28*	2.81 ± 0.19	1.95 ± 0.23*
Vastus lateralis, white (0%)	0.40 ± 0.15	0.40 ± 0.10	0.46 ± 0.07	0.44 ± 0.09	0.70 ± 0.06	0.56 ± 0.07
Vastus lateralis, mixed (11%)	1.44 ± 0.11	0.96 ± 0.13*	1.29 ± 0.17	0.81 ± 0.16*	1.67 ± 0.14	1.21 ± 0.09*
Rectus femoris, red (34%)	2.35 ± 0.26	1.62 ± 0.21*	1.92 ± 0.23	1.28 ± 0.15*	2.36 ± 0.16	1.77 ± 0.17*
Rectus femoris, white (0%)	1.05 ± 0.13	0.78 ± 0.08*	0.97 ± 0.11	0.74 ± 0.12	1.32 ± 0.07‡	0.98 ± 0.08*
Knee flexors						
Biceps femoris anterior (0%)	0.24 ± 0.03	0.28 ± 0.04	0.49 ± 0.11†	0.40 ± 0.06	0.53 ± 0.04	0.43 ± 0.05*
Biceps femoris posterior (8%)	0.76 ± 0.08	0.64 ± 0.07	0.83 ± 0.12	0.51 ± 0.11*	0.98 ± 0.09	0.70 ± 0.11*
Semitendinosus (17%)	0.55 ± 0.05	0.52 ± 0.10	0.50 ± 0.06	0.30 ± 0.03*†	0.36 ± 0.07	0.34 ± 0.06
Semimembranosus, red (28%)	0.98 ± 0.14	0.84 ± 0.09	1.20 ± 0.13	0.73 ± 0.12*	1.53 ± 0.11	1.15 ± 0.14*‡
Semimembranosus, white (0%)	0.28 ± 0.04	0.32 ± 0.04	0.40 ± 0.07	0.28 ± 0.06*	0.65 ± 0.12‡	0.51 ± 0.10*
Thigh adductors						
Adductor longus (95%)	2.85 ± 0.16	1.74 ± 0.25*	1.77 ± 0.39†	0.72 ± 0.07*†	1.94 ± 0.22	1.11 ± 0.15*
Adductor magnus & brevis (11%)	1.02 ± 0.08	0.68 ± 0.05*	0.81 ± 0.06	0.56 ± 0.16*	1.06 ± 0.13	0.80 ± 0.09*
Gracilis (23%)	0.58 ± 0.09	0.39 ± 0.04*	0.47 ± 0.07	0.37 ± 0.08	0.47 ± 0.13	0.37 ± 0.08
Pectineus (31%)	0.75 ± 0.14	0.40 ± 0.05*	0.76 ± 0.12	0.54 ± 0.10	0.56 ± 0.12	0.37 ± 0.03

Data are mean ± SEM. Values in parentheses indicate % type I + IIa according to Delp & Duan (1996). Rest; $n = 6$, Exercise; $n = 8$. *$P < 0.05$ *versus* control

Table 2-4. Effects of GLI on BF (ml min^{-1} $(100\ g)^{-1}$) and VC (ml min^{-1} $(100\ g)^{-1}$ $mmHg^{-1}$) in the kidneys and organs of the splanchnic region for rest and exercise groups.

	Rest		20		40		60	
	CON	**GLI**	**CON**	**GLI**	**CON**	**GLI**	**CON**	**GLI**
BF								
Kidney	488 ± 50	380 ± 27*	455 ± 42	417 ± 47	237 ± 107#†	164 ± 49#†	217 ± 25#†	190 ± 26#†
Stomach	100 ± 21	48 ± 8	101 ± 15	73 ± 27	86 ± 52	97 ± 72	35 ± 2	64 ± 43
Adrenals	718 ± 144	405 ± 45*	448 ± 55#	419 ± 69	253 ± 53#†	262 ± 63	217 ± 24#†	242 ± 21
Spleen	397 ± 82	307 ± 88*	113 ± 28#	115 ± 31#	27 ± 14#	21 ± 6#	25 ± 4#	16 ± 3#
Pancreas	142 ± 26	108 ± 15	198 ± 31	92 ± 22*	80 ± 27†	40 ± 9†	65 ± 7#†	38 ± 7
Sm. Intestine	304 ± 41	257 ± 37	304 ± 40	229 ± 40*	155 ± 41#†	107 ± 24#†	141 ± 8#†	88 ± 12#†
Lg. Intestine	218 ± 48	98 ± 14*	153 ± 30	116 ± 28	107 ± 35#	72 ± 23	83 ± 9#	55 ± 13
Liver**	31 ± 6	37 ± 9	20 ± 7	20 ± 6	21 ± 5	19 ± 5	26 ± 1	21 ± 3
VC								
Kidney	3.82 ± 0.50	2.53 ± 0.24*	3.30 ± 0.36	2.88 ± 0.36	1.66 ± 0.75#†	1.08 ± 0.32#†	1.53 ± 0.16#†	1.28 ± 0.18#†
Stomach	0.76 ± 0.15	0.32 ± 0.04*	0.64 ± 0.08	0.33 ± 0.05*	0.22 ± 0.06#†	0.15 ± 0.03	0.24 ± 0.01#†	0.14 ± 0.02
Adrenals	5.73 ± 1.32	2.69 ± 0.33*	3.17 ± 0.35#	2.92 ± 0.55	1.75 ± 0.40#	1.70 ± 0.40	1.52 ± 0.14#	1.61 ± 0.10
Spleen	3.08 ± 0.66	1.99 ± 0.54*	0.83 ± 0.23#	0.82 ± 0.24#	0.19 ± 0.10#	0.14 ± 0.04#	0.18 ± 0.03#	0.11 ± 0.02#
Pancreas	1.13 ± 0.22	0.72 ± 0.12*	1.46 ± 0.26	0.65 ± 0.16*	0.56 ± 0.20#†	0.26 ± 0.06	0.46 ± 0.05#†	0.25 ± 0.05
Sm. Intestine	2.35 ± 0.31	1.71 ± 0.27*	2.23 ± 0.35	1.62 ± 0.31*	1.08 ± 0.31#	0.71 ± 0.17	1.00 ± 0.05#	0.60 ± 0.09
Lg. Intestine	1.72 ± 0.38	0.64 ± 0.07*	1.11 ± 0.25#	0.90 ± 0.21	0.79 ± 0.23#†	0.50 ± 0.14#†	0.58 ± 0.06#†	0.41 ± 0.08#†
Liver**	0.24 ± 0.05	0.24 ± 0.06	0.14 ± 0.04	0.14 ± 0.04	0.14 ± 0.04	0.12 ± 0.03	0.18 ± 0.01	0.14 ± 0.02

Data are mean ± SEM. Rest; $n = 6$, Exercise; $n = 8$.*$P < 0.05$ *versus* control. **Indicates arterial, not portal, BF and VC.

Figure 2-1. GLI increased MAP (A) at rest and during submaximal exercise at 20, 40 and 60 m min^{-1} while HR (B) was decreased at rest and 20 m min^{-1}. *, $p < 0.05$ versus control.

Figure 1

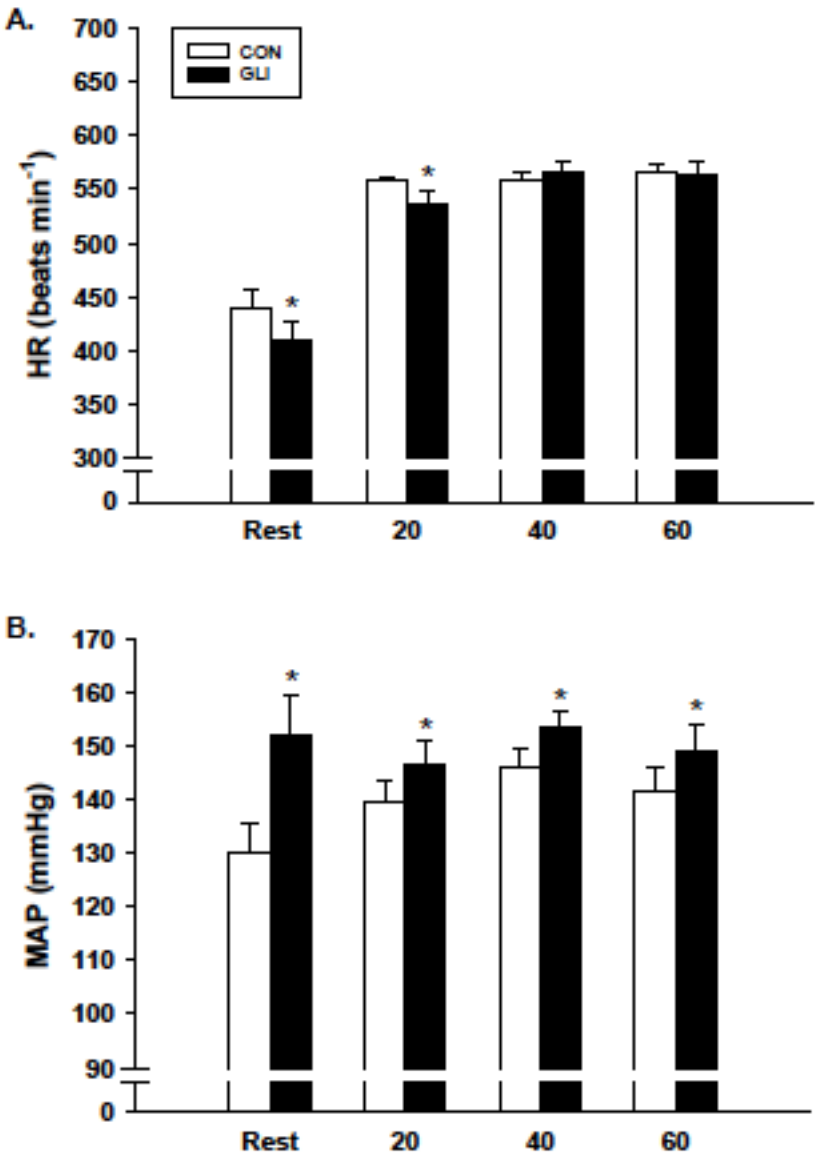

Figure 2-2. GLI decreased total hindlimb skeletal muscle BF (A) and VC (B) during submaximal exercise at 20, 40 and 60 m min^{-1} but not at rest compared to CON. *, $p < 0.05$ versus control.

Figure 2

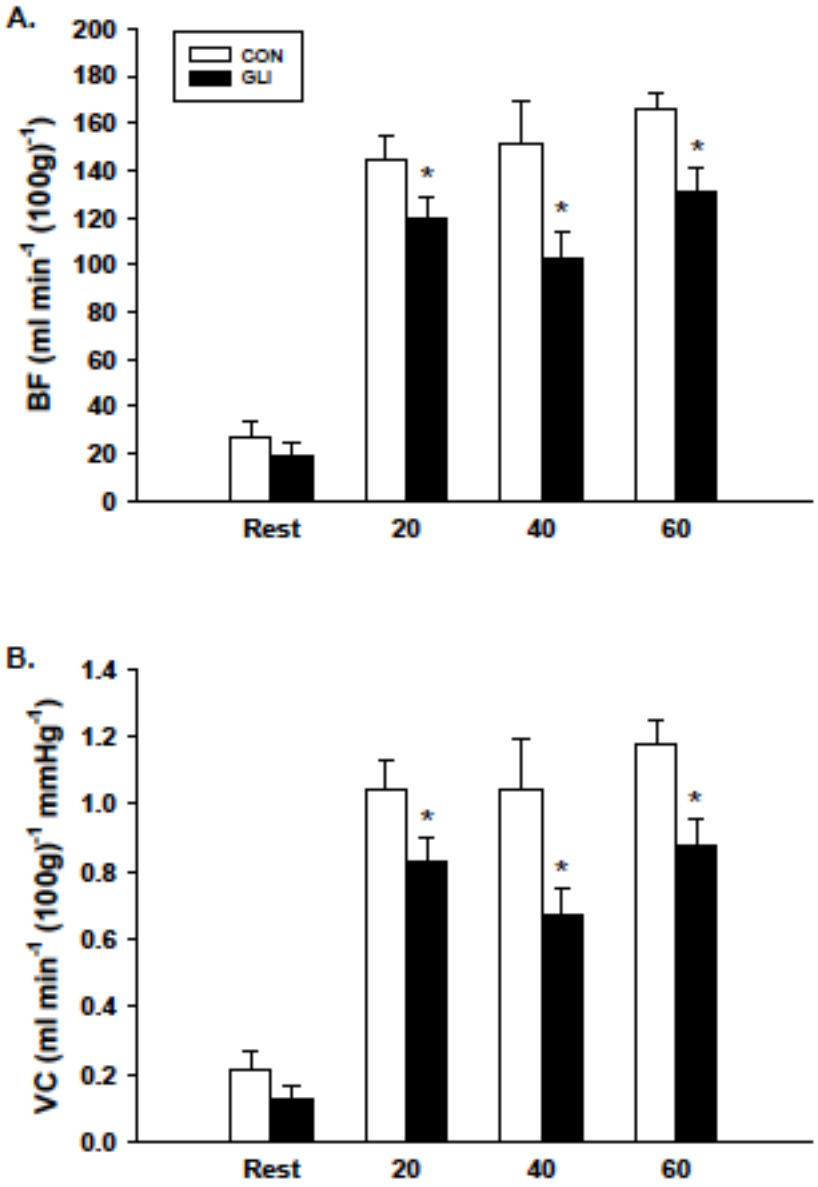

Figure 2-3. The percent decreases in exercising hindlimb VC with GLI were positively correlated with the percent type I and type IIa fibers of the muscles or muscle portions for at speeds of 20 (A), 40 (B) and 60 (C) m min^{-1}. $p < 0.05$ versus control.

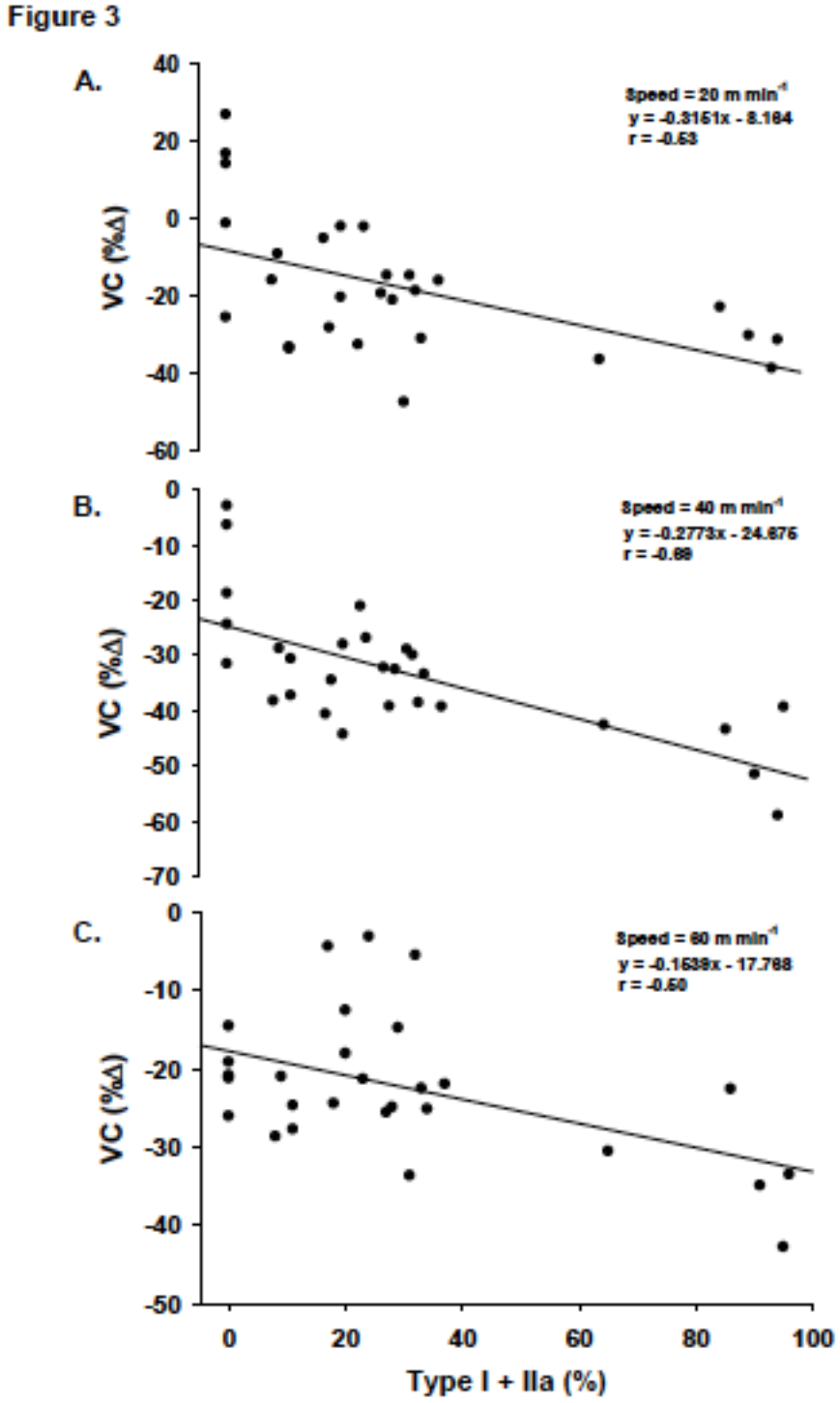

References

Bank, A.J., Sih, R., Mullen, K., Osayamwen, M., Lee, P.C., 2000. Vascular ATP-dependent potassium channels, nitric oxide, and human forearm reactive hyperaemia. Cardiovasc. Drugs Ther. 14, 23-29.

Banitt, P.F., Smits, P., Williams, S.B., Ganz, P., Creager, M.A., 1996. Activation of ATP-sensitive potassium channels contributes to reactive hyperaemia in humans. Am. J. Physiol. 271, H1594-H1598.

Beech, D.J., Zhang, H., Nakao, K., Bolton, T.B., 1993. Single channel and whole-cell K-currents evoked by levcromakalim in smooth muscle cells from the rabbit portal vein. Br. J. Pharmacol. 110, 583-590.

Beech, D.J., Zhang, H., Nakao, K., Bolton, T.B., 1993. K channel activation by nucleotidediphosphates and its inhibition by glibenclamide in vascular smooth muscle cells. Br. J. Pharmacol. 110, 573-582.

Behnke, B.J., Armstrong, R.B., Delp, M.D., 2011. Adrenergic control of vascular resistance varies in muscles composed of different fiber types: influence of the vascular endothelium. Am. J. Physiol. Regul. Integr. Comp. Physiol. 301, R783-R790.

Bijlstra, P.J., Lutterman, J.A., Russel, F.G., Thien, T., Smits, P., 1996. Interaction of sulphonylurea derivatives with vascular ATP-sensitive potassium channels in humans. Diabetologia 39, 1083-1090.

Bijlstra, P.J., den Arend, J.A., Lutterman, J.A., Russel, F.G., Thien, T., Smits, P., 1996. Blockade of vascular ATP-sensitive potassium channels reduces the vasodilator response to ischaemia in humans. Diabetologia 39, 1562-1568.

Chen, Y., Traverse, J.H., Zhang, J., Bache, R.J., 2001. Selective blockade of mitochondrial K(ATP) channels does not impair myocardial oxygen consumption. Am. J. Physiol. Heart Circ. Physiol. 281, H738-H744.

Cole, W.C., Clément-Chomienne, O., 2003. ATP-sensitive K+ channels of vascular smooth muscle cells. J. Cardiovasc. Electrophysiol. 14, 94-103.

Copp, S.W., Hirai, D.M., Hageman, K.S., Poole, D.C., Musch, T.I., 2010. Nitric oxide synthase inhibition during treadmill exercise reveals fiber-type specific vascular control in the rat hindlimb. Am. J. Physiol. Regul. Integr. Comp. Physiol. 298, R478-R485.

Comtois, A., Sinderby, C., Comtois, N., Grassino, A., Renaud, J.M., 1994. An ATP-sensitive potassium channel blocker decreases diaphragmatic circulation in anesthetized dogs. J. Appl. Physiol. 77, 127-134.

Cunha, M.R., Silva, M.E., Machado, H.A., Fukui, R.T., Correia, M.R., Santos, R.F., Wajchenberg, B.L., Rocha, D.M., Rondon, M.U., Negrão, C.E., Ursich, M.J., 2008. Cardiovascular, metabolic and hormonal responses to the progressive exercise performed to exhaustion in patients with type 2 diabetes treated with metformin or glyburide. Diabetes Obes. Metab. 10, 238-245.

Delp, M.D., Duan, C., 1996. Composition and size of type I, IIA, IID/X, and IIB fibers and citrate synthase activity of rat muscle. J. Appl. Physiol. 80, 261-270.

Dinenno, F.A., Joyner, M.J., 2004. Combined NO and PG inhibition augments α-adrenergic vasoconstriction in contracting human skeletal muscle. Am. J. Physiol. Heart Circ. Physiol. 287, H2576-H2584.

Drummond, G.B., 2009. Reporting ethical matters in The Journal of Physiology: standards and advice. J. Physiol. 587, 713–719.

Duncker, D.J., Oei, H.H., Hu, F., Stubenitsky, R., Verdouw, P.D., 2001. Role of K+ATP channels in regulation of systemic, pulmonary, and coronary vasomotor tone in exercising swine. Am. J. Physiol. Heart Circ. Physiol. 280, H22-H33.

Farouque, H.M., Meredith, I.T., 2003. Effects of inhibition of ATP-sensitive potassium channels on metabolic vasodilation in the human forearm. Clin. Sci. 104, 39-46.

Gardiner, S.M., Kemp, P.A., March, J.E., Fallgren, B., Bennet, T., 1996. Effects of glibenclamide on the regional haemodynamic actions of α-trinositol and its influence on responses to vasodilators in conscious rats. Br. J. Pharmacol. 117, 507-515.

George, S., McBurney, A., Cole, A., 1990. Possible protein binding displacement interaction between glibenclamide and metolazone. Eur. J. Clin. Pharmacol. 38, 93–95.

Guo, Q., Jin, S., Wang, X.L., Wang, R., Xiao, L., He, R.R., Wu, Y.M., 2011. Hydrogen sulfide in the rostral ventrolateral medulla inhibits sympathetic vasomotor tone through ATP-sensitive K+ channels. J. Pharmacol. Exp. Ther. 338, 458-465.

Hellsten, Y., Nyberg, M., Jensen, L.G., Mortensen, S.P., 2012. Vasodilator interactions in skeletal muscle blood flow regulation. J. Physiol. 590, 6297-6305.

Hirai, T., Visneski, M.D., Kearns, K.J., Zelis, R., Musch, T.I., 1994. Effects of NO synthase inhibition on the muscular blood flow response to treadmill exercise in rats. J. Appl. Physiol. 77, 1288-1293.

Ishise, S., Pegram, B.L., Yamamoto, J., Kitamura, Y., Frohlich, E.D., 1980. Reference sample microsphere method: cardiac output and blood flows in conscious rat. Am. J. Physiol. 239, H443-H449.

Jackson, W.F., 2005. Arteriolar tone is determined by activity of ATP-sensitive potassium channels. Am. J. Physiol. 265, H1797-H1803.

Larsen, J.J., Dela, F., Madsbad, S., Vibe-Petersen, J., Galbo H., 1999. Interaction of sulfonylureas and exercise on glucose homeostasis in type 2 diabetic patients. Diabetes Care. 22, 1647-1654.

Malester, B., Tong, X., Ghiu, I., Kontogeorgis, A., Gutstein, D.E., Xu, J., Hendricks-Munoz, K.D., Coetzee, W.A., 2007. Transgenic expression of a dominant negative K(ATP) channel subunit in the mouse endothelium: effects on coronary flow and endothelin-1 secretion. FASEB J. 21, 2162-2172.

Mori, H.M., Chujo, M., Tanaka, E., Yamakawa, A., Shinozaki, Y., Mohamed, M.U., Nakazawa, H., 1995. Modulation of adrenergic coronary vasoconstriction via ATP-sensitive potassium channel. Am. J. Physiol. 268, H1077-H1085.

Moreau, R., Komeichi, H., Kirstetter, P., Yang, S., Aupetit-Faisant, B., Cailmail, S., Lebrec, D., 1994. Effects of glibenclamide on systemic and splanchnic haemodynamics in conscious rats. Br J. Pharmacol. 112, 649-653.

Murphy, M.E., Brayden, J.E., 1995. Nitric oxide hyperpolarizes rabbit mesenteric arteries via ATP-sensitive potassium channels. J. Physiol. 486, 47-58.

Musch, T.I., Terrell, J.A. 1992. Skeletal muscle blood flow abnormalities in rats with a chronic myocardial infarction: rest and exercise. Am. J. Physiol. 262, H411-H419.

Nakai, T., Ichihara, K., 1994. Effects of diazoxide on norepinephrine-induced vasocontraction and ischemic myocardium in rats. Biol. Pharmacol. Bull. 17, 1341-1344.

Nelson, M.T., Patlak, J.B., Worley, J.F., Standen, N.B., 1990. Calcium channels, potassium channels, and voltage dependence of arterial smooth muscle tone. Am. J. Physiol. 259, C3-C18.

Nelson, M.T., Quayle, J.M., 1995. Physiological roles and properties of potassium channels in arterial smooth muscle. Am. J. Physiol. 268, C799-C822.

Nielsen, J.J., Kristensen, M., Hellsten, Y., Bangsbo, J., Juel, C., 2003. Localization and function of ATP-sensitive potassium channels in human skeletal muscle. Am. J. Physiol. Regul. Integr. Comp. Physiol. 284, R558-R563.

Padilla, D.J., McDonough, P., Behnke, B.J., Kano, Y., Hageman, K.S., Musch, T.I., Poole, D.C., 2007. Effects of Type II diabetes on muscle microvascular oxygen pressures. Respir. Physiol. Neurobiol. 156, 187-195.

Parekh, N., Zou, A.P., 1996. Role of prostaglandins in renal medullary circulation: response to different vasoconstrictors. Am. J. Physiol. 271, F653-F658.

Poole, D.C., Ferreira, L.F., 2007. Oxygen exchange in muscle of young and old rats: muscle-vascular-pulmonary coupling. Exp. Physiol. 92, 341–346.

Poole, D.C., Hirai, D.M., Copp, S.W., Musch, T.I., 2012. Muscle oxygen transport and utilization in heart failure: implications for exercise (in)tolerance. Am. J. Physiol. Heart Circul. Physiol. 302, H1050-H1063.

Quast, U., Guillon, J.M., Cavero, I., 1994. Cellular pharmacology of potassium channel openers in vascular smooth muscle. Cardiovasc. Res. 28, 805-810.

Saito, Y., McKay, M., Eraslan, A., Hester, R.L., 1996. Functional hyperaemia in striated muscle is reduced following blockade of ATP-sensitive potassium channels. Am. J. Physiol. Heart Circ. Physiol. 270, H1649-H1654.

Sadraei, H., Beech, D.J., 1995. Ionic currents and inhibitory effects of glibenclamide in seminal vesicle smooth muscle cells. Br. J. Pharmacol. 115, 1447-1454.

Schrage, W.G., Dietz, N.M., Joyner, M.J., 2006. Effects of combined inhibition of ATP-sensitive potassium channels, nitric oxide, and prostaglandins on hyperaemia during moderate exercise. J. Appl. Physiol. 100, 1506-1512.

Symons, J.D., Stebbins, C.L., Musch, T.I., 1999. Interactions between angiotensin II and nitric oxide during exercise in normal and heart failure rats. J. Appl. Physiol. 87, 574-581.

Tare, M., Parkington, H.C., Coleman, H.A., Neild, T.O., Dusting, G.J., 1990. Hyperpolarization and relaxation of arterial smooth muscle caused by nitric oxide derived from the endothelium. Nature. 346, 69-71.

Tateishi, J., Faber, J.E., 1995. ATP-sensitive K+ channels mediate α2D-adrenergic receptor contraction of arteriolar smooth muscle and reversal of contraction in hypoxia. Circ. Res. 76, 53-63.

Teramoto, N., 2006. Physiological roles of ATP-sensitive K+ channels in smooth muscle. J. Physiol. 572, 617-624.

Thomas, G.D., Hansen, J., Victor, R.G., 1997. ATP-sensitive potassium channels mediate contraction-induced attenuation of sympathetic vasoconstriction in rat skeletal muscle. J. Clin. Invest. 99, 2602-2609.

Vanelli, G., Hussain, S.N., 1994. Effects of potassium channel blockers on basal vascular tone and reactive hyperaemia of canine diaphragm. Am. J. Physiol. 266, H43-H51.

Chapter 3 - Modulation of rat skeletal muscle microvascular O_2 pressure via K_{ATP} channel inhibition following the onset of contractions

Abstract

Vascular hyperpolarization mediated, in part, by the ATP-sensitive K^+ (K_{ATP}) channel contributes to exercise-induced increases in skeletal muscle O_2 delivery. We hypothesized that K_{ATP} channel inhibition via glibenclamide (GLI) would speed the fall of microvascular O_2 driving pressure (PO_2mv; set by the O_2 delivery-O_2 utilization ratio), during muscle contractions. Spinotrapezius muscle PO_2mv (phosphorescence quenching) was measured in 12 adult Sprague Dawley rats during 180 s of 1-Hz twitch contractions (~6 V) under control and GLI (5 mg/kg) conditions. The total mean PO_2mv response time was greater with GLI (i.e. slowed; control: 42.0 ± 14.2, GLI: 79.5 ± 14.7 s, $p < 0.05$). A clear undershoot of the contracting steady-state PO_2mv was evident with GLI (15.6 ± 5.3 %, $p < 0.05$) but not control (2.3 ± 1.6 %, $p > 0.05$). This indicates that K_{ATP} channel inhibition does not speed PO_2mv kinetics per se during small muscle mass contraction. However, it does induce a transient mismatch of O_2 delivery-O_2 utilization, lowers PO_2mv, and delays attainment of the contracting steady-state.

Introduction

The transport of O_2 from alveoli in the lung to skeletal muscle mitochondria involves pressure-driven delivery across multiple resistances in series. Vitally important among these gradients is the pressure head driving O_2 from capillary blood to skeletal myocytes which is determined by the microvascular oxygen pressure (PO_2mv) in accordance with Fick's Law of diffusion. The PO_2mv is set by the ratio of O_2 delivery ($\dot{Q}O_2$) to O_2 utilization ($\dot{V}O_2$) and, at the onset of contractions, this pressure provides a fundamental characterization of temporal O_2 delivery as it attempts to match near-instantaneous increases in O_2 demand (Behnke et al., 2002; Ferreira et al., 2005). Fortunately, in healthy individuals the mechanical, neural and humoral mechanisms of vascular control are capable of producing remarkably fast muscle O_2 delivery kinetics to maintain an adequate PO_2mv during the metabolic transients of daily activity (rev. Heinonen et al., 2015; Joyner and Casey, 2015). This function is essential given that even a brief mismatch of O_2 delivery-to-utilization at the onset of exercise can cause a premature decline in muscle PCr stores and the accumulation of muscle metabolites associated with fatigue such as ADP, H^+, K^+ and P_i (Hogan et al., 1992; Richardson et al., 1995; Wilson et al., 1977).

Vasomotor sensitivity to depolarization depends upon the membrane potential of vascular smooth muscle cells and thus the modulation of membrane potential may represent an important mechanism contributing to the kinetics of vascular control and skeletal muscle O_2 delivery during exercise. The vascular ATP-sensitive K^+ (K_{ATP}) channel subtype is a nucleotide-dependent, inward rectifier K^+ channel (Kir) that is activated, in part, by the accumulation of subsarcolemmal ADP (Beech et al., 1993). The K_{ATP} channel may therefore help coordinate local O_2 availability and vasomotor tone across the greater-than-two orders of magnitude increase in muscle metabolism seen with exercise. K_{ATP} channel activation elicits the smooth muscle

hyperpolarization characteristic of Kir channels, resulting in the relaxation of smooth muscle and attenuated α-adrenergic vasoconstriction (Keller et al., 2004; Nakai and Ichihara, 1994; Tateishi and Faber, 1995). The ability to couple vascular tone with cellular metabolism makes the K_{ATP} channel a strong candidate for contributing to the increased O_2 delivery at the onset of contractions. In vivo investigations of K_{ATP} channel function are equivocal; some demonstrating robust effects on the magnitude of the hyperemic response at steady-state (Banitt et al., 1996; Bank et al., 2000; Bijlstra et al., 1996; Holdsworth et al., 2015) while others find no change (Duncker et al., 2001; Farouque and Meredith, 2003; Schrage et al., 2006). These disparate findings may belie an important K_{ATP} channel contribution to the speed, rather than magnitude, of the hyperemic response under specific circumstances (i.e. muscle mass, oxidative capacity, exercise intensity, etc.). Indeed, because of the redundancy of vasodilatory mediators the eventual attainment of steady-state PO_2mv might be anticipated irrespective of the participation of K_{ATP} channels, or not, in the exercise hyperemia (Clifford and Hellsten, 2004).

The tight regulation of O_2 delivery to O_2 utilization across the metabolic transition has historically been credited as a dominant feature of the exercise response (Krogh and Lindhard, 1913; rev. Poole and Jones, 2012). Hence careful examination of the contraction-induced muscle PO_2mv kinetics prior to the attainment of a steady-state is obligatory to understanding the role(s) of vascular K_{ATP} channel function in vivo. The purpose of the present investigation was to test the hypothesis that inhibition of K_{ATP} channels via glibenclamide (GLI) in healthy rats would 1) accelerate the fall of PO_2mv following the onset spinotrapezius muscle contractions and 2) result in a lower mean PO_2mv during the total duration of contractions.

Methods

Ethical approval

All procedures were approved by the Institutional Animal Care and Use Committee of Kansas State University under the guidelines established by the National Institutes of Health. 12 adult male Sprague-Dawley rats (~4 months old) were maintained in accredited animal facilities (Association for the Assessment and Accreditation of Laboratory Animal Care) at Kansas State University on a 12-h light/12-h dark cycle with food and water provided *ad libitum*.

Drugs

The pharmacological sulphonylurea derivative GLI (494 g mol^{-1}; 5-chloro-*N*-(4-[*N*-(cyclohexylcarbamoyl)sulfamoyl]phenethyl)-2-methoxybenzamide; Sigma-Aldrich, St Louis, MO, USA) was used to inhibit vascular K_{ATP} channels. Briefly, 25 mg of GLI was dissolved in 99:1 ratio of saline/NaOH (1.0 M) to produce a 2.5 mg ml^{-1} stock solution. A 5 mg kg^{-1} dose was drawn from the stock solution and diluted to ~1 ml with heparinized saline. It has been reported previously that GLI is a selective K_{ATP} channel blocker at concentrations below 5 µmol L^{-1} (Beech et al., 1993; Sadraei and Beech, 1995). The current dose of 5 mg kg^{-1} for rats of a mean body mass of 366 g equates to a blood concentration of ~140 µmol L^{-1}. Given that 98-99% of GLI is bound to plasma protein, the effective blood concentration of GLI is ~2-3 µmol L^{-1} (George et al., 1990) which is in the range for GLI to be selective for K_{ATP} channels without inhibition of Ca^{2+} channel current (Sadraei and Beech, 1995). This dosing strategy, based on smooth muscle cell investigations, was shown to elicit a degree of K_{ATP} channel block for swine in vivo (Duncker et al., 2001). See Discussion for further considerations of K_{ATP} channel inhibition.

Surgical instrumentation

On the day of the final protocol the rats were anesthetized initially with a 5% isoflurane-O_2 mixture and maintained on a 3% isoflurane-O_2 mixture for the duration of the surgical instrumentation. The carotid artery was cannulated with PE-10 connected to PE-50 (Intra-Medic polyethylene tubing, BD, Franklin Lakes, NJ, USA) for the measurement of mean arterial pressure (MAP) and heart rate (HR) as well as infusion of the phosphorescent probe G2. A caudal artery catheter was placed for blood sampling and administration of anesthetics. Isoflurane-O_2 inhalation was progressively removed as anesthesia was maintained with pentobarbital sodium administered via the caudal artery catheter to effect. Depth of anesthesia was monitored at frequent and regular intervals via the blink and toe-pinch reflexes as well as magnitude and frequency of ventilation. Access to the spinotrapezius was achieved by surgically reflecting the overlying skin and fascia. The spinotrapezius muscle was selected because the fiber-type composition and oxidative capacity closely resembles that of the human quadriceps muscle group which makes it a useful analog of human locomotor muscle (Delp and Duan, 1996). During both the surgical preparation and experimental protocol the muscle was superfused frequently with Krebs-Hensleit bicarbonate-buffered solution consisting of (in mM) 4.7 KCl, 2.0 $CaCl_2$, 2.4 $MgSO_4$, 131 NaCl, and 22 $NaHCO_3$ equilibrated with 5% CO_2 and 95% N_2 (pH 7.4, 37-38°C). Exposed tissue surrounding the spinotrapezius muscle was covered with Saran wrap (Dow Brands, Indianapolis, IN) to reduce dehydration and limit exposure of GLI to the spinotrapezius only. Stainless steel electrodes were sutured to the rostral (cathode) and caudal (anode) regions of the spinotrapezius muscle for electrically-induced twitch contractions. As previously reported by our laboratory these surgical procedures do not impact the microvascular integrity and responsiveness of the rat spinotrapezius muscle (Bailey et al., 2000).

Experimental protocol

Two separate contraction bouts were performed under control (saline/NaOH vehicle, i.a.) and GLI (5 mg/kg, i.a.) conditions. The vehicle (~1 ml) was administered for control via the caudal artery catheter followed by a 180 s muscle PO_2mv recording. After a 1-3 minute period to ensure that baseline PO_2mv had stabilized, muscle contraction was evoked via electrical stimulation (1 Hz, ~6 V, 2-ms pulse duration, model s48; Grass Technologies, Quincy, MA) for 180 s. This protocol has been shown to increase blood flow four- to five-fold and metabolic rate six- to seven-fold without altering blood pH and is consistent with moderate intensity exercise (Behnke et al., 2002; Hirai et al., 2013). Immediately upon cessation of electrical stimulation an arterial blood sample was drawn (~0.8 ml) for the determination of blood gases, hematocrit, pH, [lactate] and [glucose]. After a ~25 min recovery the second contraction bout was performed in an identical fashion to the first after the administration of GLI (5 mg/kg). As previously reported by our laboratory, >20 min recovery elicits reproducible PO_2mv responses (Copp et al., 2009; Herspring et al., 2008). At the end of the protocol, rats were euthanized with intra-arterial pentobarbital sodium overdose (>50 mg/kg) and subsequent removal of the heart.

Spinotrapezius PO_2mv measurement

PO_2mv was measured via phosphorescence quenching using a frequency domain phosphorometer (PMOD 5000; Oxygen Enterprises, Philadelphia, PA). As described previously (Behnke et al., 2001), this technique applies the Stern-Volmer relationship (Rumsey et al., 1988), which describes the quantitative O_2 dependence of the phosphorescent probe G2 via the equation:

$$PO_2mv = [(\tau^\circ/\tau) - 1]/(k_Q \cdot \tau^\circ)$$

where k_Q is the quenching constant and τ and $\tau°$ are the phosphorescence lifetimes at the ambient O_2 concentration and in the absence of O_2, respectively. For the phosphorescent probe G2, k_Q is 273 $mmHg^{-1}$ s^{-1} and $\tau°$ is 251 μs (Bodmer et al., 2012; Dunphy et al., 2002). These characteristics do not change over the physiological range of pH (~7.4) and temperature (~38°C) *in vivo* and, therefore, the phosphorescence lifetime is affected solely by the O_2 partial pressure. The Pd-porphyrin cores of phosphor probes bind to albumin; the primary macromolecule in plasma. This quality as well as the probes' negative charge ensures restriction to the vascular compartment, of which, the capillary bed volumetrically constitutes the major intramuscular space (Poole et al., 2004). After infusion of G2 the common end of the bifurcated light guide with a >500 μm penetration depth was positioned ~2-4 mm superficial to the dorsal surface of the exposed spinotrapezius muscle in an area devoid of macro-vessels. The phosphorometer modulates sinusoidal excitation frequencies between 100 Hz and 20 kHz and allows phosphorescence lifetime measurements from 10 μs to ~2.5 ms. PO_2mv was measured continuously and recorded at 2-s intervals throughout the duration of the experimental protocol.

Analysis of spinotrapezius PO_2mv kinetics

PO_2mv time course was determined via exponential regression analysis by applying the Levenberg-Marquardt algorithm (SigmaPlot 11.0; Systat software, San Jose, CA) to the contraction-induced PO_2mv transient. The sum of squared residuals was used to indicate the appropriateness of the model fit. PO_2mv responses were fit with either a one- or two-component model as follows.

One component:

$$PO_2mv_{(t)} = PO_2mv_{(BL)} - \Delta PO_2mv\ (1 - e^{-(t - TD)/\tau})$$

Two component:

$$PO_2mv_{(t)} = PO_2mv_{(BL)} - \Delta_1 PO_2mv\ (1 - e^{-(t - TD_1)/\tau_1}) + \Delta_2 PO_2mv\ (1 - e^{-(t - TD_2)/\tau_2})$$

$PO_2mv_{(t)}$ is the PO_2mv at a given time *t*; $PO_2mv_{(BL)}$ corresponds to the pre-contracting resting PO_2mv; Δ_1 and Δ_2 are the amplitudes for the first and second components, respectively; TD_1 and TD_2 are the independent time delays for each component; and τ_1 and τ_2 are the time constants (i.e. time to 63% of the response) for each component. Goodness of fit was determined using three criteria: the coefficient of determination, sum of squared residuals, and visual inspection (Behnke et al., 2002).

The mean response time (MRT_1) was used to describe the overall dynamics of the PO_2mv fall following the onset of muscle contractions via the equation:

$$MRT_1 = TD_1 + \tau_1$$

The MRT_1 analysis was limited to the first component of the PO_2mv response given that inclusion of an emergent second component underestimates the speed of the PO_2mv fall at the onset of contractions. In the event of a second component the MRT_2 was calculated using the following equation:

$$MRT_2 = TD_2 + \tau_2$$

To determine the overall time taken to reach the steady-state PO_2mv the MRT_{Total} was calculated via the equation:

$$MRT_{Total} = MRT_1 + MRT_2$$

The MRT_{Total} does not equal the sum of the MRT_1 and MRT_2 averages because MRT_2 is independent of the calculation of MRT_{Total}. The purpose of the second component kinetics parameters is to represent the speed with which the $PO_2mv_{(SS)}$ is reached after the initial fall in PO_2mv. For this reason, the MRT_2 averages are calculated from rats with a two-component fit

only. However, the calculation of MRT_{Total} necessarily reflects the absence of MRT_2 (i.e. effectively zero) for rats fit with a one-component model.

Statistical analysis

MAP and HR were compared between conditions and across time points via 2-way repeated measures ANOVA. The frequency of the PO_2mv undershoot was determined via a chi-squared test. All other results were compared between conditions with paired Student's *t*-tests. The level of significance was set at $p < 0.05$. Results are presented as means ± SE.

Results

Arterial blood samples and cardiovascular hemodynamics

Arterial PO_2, PCO_2, O_2 saturation, hematocrit and pH were not different between conditions ($p > 0.05$) which was also the case for arterial blood [lactate] (control: 1.4 ± 0.1, GLI: 1.5 ± 0.2 mmol/L, $p > 0.05$) and [glucose] (control: 70 ± 7, GLI: 108 ± 17 mg/dL, $p > 0.05$). MAP was increased by GLI (Pre: 104 ± 4, Post: 121 ± 4 mmHg, $p < 0.05$) but not control infusion (Pre: 94 ± 5, Post: 96 ± 5 mmHg, $p > 0.05$). HR was not different with GLI (Pre: 348 ± 15, Post: 339 ± 15 bpm, $p > 0.05$) or control infusion (Pre: 349 ± 7, Post: 352 ± 7 bpm, $p > 0.05$).

Spinotrapezius PO_2mv

There was no difference in PO_2mv between pre- and post-GLI or pre- and post-control ($p > 0.05$; Fig. 1). However, GLI (Pre: 33.3 ± 1.7, Peak: 40.2 ± 1.5 mmHg, $p < 0.05$) but not control (Pre: 33.8 ± 2.0, Peak: 35.0 ± 2.2 mmHg, $p > 0.05$) caused a transient increase in spinotrapezius PO_2mv that returned to baseline by 180 s (Fig. 1). Neither baseline nor steady-state contracting spinotrapezius PO_2mv were different with GLI infusion (Table 1). During the control condition 2 of 12 rats exhibited PO_2mv profiles that transiently fell below the contracting steady-state (termed an "undershoot", $\Delta_2PO_2$mv) necessitating a two-component model fit. Conversely, during GLI the two-component model was required for 7 of 12 rats. The goodness of fit for the two-component model was not different for r^2 (control: 0.98 ± 0.01, GLI: 0.98 ± 0.00, $p > 0.05$) or the sum of squared residuals (control: 19.0 ± 5.9, GLI: 23.0 ± 7.0, $p > 0.05$) between conditions. The individual changes in $\Delta_2PO_2$mv for these rats are highlighted in Figure 2B demonstrating the values during control and GLI trials. Note the increase in the magnitude of GLI $\Delta_2PO_2$mv for the two rats with undershoots present in the control condition. Using the control outcomes (2/12) as the expectation, a chi-squared analysis revealed that GLI increased

the frequency of an undershoot occurrence in PO_2mv during contractions ($p < 0.01$). The undershoot magnitude as a percentage of both steady-state (control: 1.6 ± 1.1, GLI: 8.0 ± 2.6 %, $p < 0.05$) and the overall amplitude of the response (control: 2.3 ± 1.6, GLI: 15.6 ± 5.3 %, $p < 0.05$) was greater with GLI (Fig. 2C). Furthermore, at the onset of contractions no parameters characterizing the fall in PO_2mv were different between control and GLI ($p > 0.05$). However, due to the more pronounced undershoot the total MRT (MRT_{Total}; $MRT_1 + MRT_2$) was increased with GLI (control: 42.0 ± 14.2, GLI: 79.5 ± 14.7 s, $p < 0.05$). The result was a significant reduction in the mean PO_2mv ($p < 0.001$) over the total duration of contractions which was particularly evident between 30 and 60 seconds (Δ: 1.2 ± 0.05 mmHg).

Discussion

These data indicate that, in contrast to our hypothesis, GLI does not speed the fall in PO_2mv at the onset of contractions but does increase the occurrence of PO_2mv undershoots wherein PO_2mv falls initially below the steady state. At some 30-60 seconds of contractions a presumably more sluggish increase in $\dot{Q}O_2$ concomitant with the mono-exponential rise in muscle $\dot{V}O_2$ (Behnke et al., 2002) drives PO_2mv lower (~15% of the total amplitude) prior to the attainment of the steady state. This phenomenon affects the PO_2mv profile by 1) nearly doubling the time to reach the steady state from the onset of contractions (i.e. MRT_{Total}; 190% of the control condition) and 2) further reducing the mean PO_2mv, the magnitude of which represents a modest ~11% of the fall in PO_2mv ($\Delta_1PO_2$mv). The combination of an increased undershoot occurrence, increased overall mean response time, and reduced mean PO_2mv with GLI suggests that the K_{ATP} channel regulates, in part, the PO_2mv at the onset of contractions in healthy rat spinotrapezius muscle. Furthermore, the decrement in blood-myocyte O_2 driving pressure coincides closely with the rapid, phase II rise in muscle $\dot{V}O_2$ which may contribute to a slowing of $\dot{V}O_2$ kinetics.

K_{ATP} channel inhibition and cardiovascular hemodynamics

As expected the intra-arterial administration of GLI increased MAP and reduced HR compared to infusion of the vehicle. This robust increase in MAP has been shown to result from a decreased conductance in the renal and splanchnic vascular beds (Duncker et al., 2001; Holdsworth et al., 2015). The role of the K_{ATP} channel in setting basal vasomotor tone is well established and the inability of the baroreflex to prevent the GLI-induced rise in MAP supports the obligatory function of the K_{ATP} channel in systemic vascular control. Crucially,

administration of the vehicle did not significantly alter MAP which indicates a primary effect of GLI rather than a volume-loading response.

K_{ATP} channel inhibition and spinotrapezius PO_2mv

As seen in Figure 1 GLI infusion produced a transient increase in PO_2mv which returned to pre-infusion levels such that baseline PO_2mv was not different between conditions. This rise was coincident with a large increase in central driving pressure (i.e. % increase in MAP) due to vasoconstriction of quiescent tissue as described above. The ability to match O_2 delivery to O_2 utilization after this brief transient (2-3 min) is not surprising given the redundant parallel pathways for skeletal muscle vasomotor control (e.g. NO, prostacyclin, baroreflex, myogenic control) to maintain appropriate O_2 delivery, particularly at rest (Clifford and Hellsten, 2004). Indeed, measures of skeletal muscle blood flow at rest are unchanged with K_{ATP} channel inhibition for the rat (Holdsworth et al., 2015), pig (Duncker et al., 2001) and human (Farouque and Meredith, 2003) which is in line with the findings herein.

The spinotrapezius PO_2mv profiles herein are consistent with those demonstrated previously by our laboratory in healthy rats (Behnke et al., 2001). K_{ATP} channel manipulation of the steady-state $\dot{Q}O_2$ has been characterized previously for in vivo electrical stimulations (Thomas et al., 1997), reactive hyperemia (Banitt et al., 1996; Bank et al., 2000; Bijlstra et al., 1996) and exercise-induced hyperemia (Holdsworth et al., 2015). Our findings expand upon these investigations by demonstrating that, with GLI, the development of a PO_2mv undershoot reduces the mean PO_2mv during contractions and prolongs the overall time to achieve the contracting steady-state PO_2mv. This reduced skeletal muscle PO_2mv with GLI may impair blood-tissue O_2 flux, decrease intracellular PO_2 and elevate the accumulation of metabolites

implicated in fatigue (i.e. ADP, H^+, P_i, K^+) (Arthur et al., 1992; Hogan et al., 1992), thereby diminishing exercise tolerance (Grassi et al., 2015; Poole et al., 2012).

The K_{ATP} channel inhibition may not have been complete and therefore the lower mean PO_2mv and higher time to achieve steady-state PO_2mv with GLI may be underestimated. The magnitude of the effect should also be considered in the context of varying skeletal muscle metabolic characteristics. The rat spinotrapezius demonstrates a mosaic fiber-type which is distributed approximately equally between low and high oxidative fiber types. Differential effects with K_{ATP} channel inhibition may be found across other more distinctly fiber-type compartmentalized muscles common to the rat. Our recent data suggests that the role of the K_{ATP} channel in muscle O_2 delivery is fiber-type dependent with the GLI-induced reductions seen predominantly in highly oxidative muscles and muscle portions (Holdsworth et al., 2015). Thus, in mixed fiber-type muscles a less pronounced effect of K_{ATP} channel inhibition on the PO_2mv profile may be observed, reinforcing the notion that a significant role for K_{ATP} channel function in exercise-induced hyperemia is driven by muscles with a dominant type I and IIa fiber composition. Despite the possible underestimation of effects due to these experimental considerations, the contraction-induced PO_2mv profile with K_{ATP} channel inhibition does reflect a characteristic undershoot and prolonged recovery to the final contracting steady-state in the spinotrapezius which provides the closest translation to human locomotory muscle. This function of the K_{ATP} channel should not be underestimated given that the PO_2mv undershoot and delayed steady state are well-defined in O_2 supply-limited conditions such as heart failure (Ferreira et al., 2006a), aging (Behnke et al., 2005) and diabetes mellitus (Padilla et al., 2007) which also present with severe exercise intolerance (Piepoli et al., 2010a, 2010b; Sacre et al., 2015).

The PO_2mv undershoot has been attributed, in part, to reductions in NO-bioavailability (Ferreira et al., 2006a, 2006b). The parallel role of K_{ATP} channels and NO in manifesting the PO_2mv undershoot highlights the plausible synergism between these two mediators of vasodilation. NO has been shown to cause arterial hyperpolarization, in part, via K_{ATP} channel activation (Murphy and Brayden, 1995) which may occur through the cGMP intermediary that elicits K_{ATP} channel activation in cardiac myocytes (Chai et al., 2011) and cultured smooth muscle cells (Kubo et al., 1994). Furthermore, as a reactive nitrogen species, NO can cause direct S-nitrosylation of cysteine residues found on the SURx subunit (Kawano et al., 2009; Yoshida et al., 2006), and channel activation via NO is likely mediated through a combination of the two mechanisms. The notion that K_{ATP} channels can act as an amplifier for NO and other vasoactive signals (Cole et al., 2000; Silva et al., 2008) via modulation of membrane potential deserves further investigation and may be valuable clinically (reviewed by Akrouh et al., 2009).

Implications for sulphonylurea therapy

The schema presented herein is cause for concern given the use of sulphonylureas in the treatment of diabetes. Recently, the American College of Physicians has scrutinized the administration of sulphonylureas as a first-line monotherapy in diabetes, and the current treatment guidelines dictate that their use be reserved for cases where lifestyle modifications to diet and physical activity have proved ineffective (Qaseem et al., 2012). In support of this consensus, large retrospective studies revealed the associative risk of cardiovascular mortality and morbidity with sulphonylurea monotherapy (Fadini et al., 2015; Morgan et al., 2014; Simpson et al., 2006). In this regard, our findings demonstrate a significant peripheral vascular dysfunction with GLI which would be easily overlooked in the absence of overt cardiovascular disease (e.g. heart failure) or cardiovascular events (e.g. myocardial infarct, severe angina).

Interestingly, the reduced blood-myocyte O_2 driving pressure appears to be time-aligned with the rapid phase II increase in muscle $\dot{V}O_2$ following the initiation of exercise (Behnke et al., 2002). The phase II muscle $\dot{V}O_2$ kinetics are significantly slowed in diabetic patients and an intriguing question is whether it is a diabetes- or sulphonlyurea-induced dysfunction of the K_{ATP} channel that is associated with the $\dot{V}O_2$ kinetics limitation (Bauer et al., 2007; O'Connor et al., 2015; Regensteiner et al., 1998). The answer is crucial for a diabetic population with compromised vascular function and reduced work capacity where an additional drag on O_2 delivery could be the tipping point for patient quality of life.

Experimental considerations

The exaggerated fall in skeletal muscle PO_2mv at the onset of contractions is mediated by a non-proportional increase in the O_2 delivery and utilization components of this ratio. Importantly, it must be considered whether a GLI-mediated increase in $\dot{V}O_2$ is plausible and, if so, whether it may be the principal driver of the PO_2mv profile alterations seen herein. Despite the absence of a specific mitochondrial K_{ATP} channel blocker, the available evidence *in vivo* suggests that there is no change in $\dot{V}O_2$ during whole body exercise (Larsen et al., 1999) with GLI and that mitochondrial K_{ATP} channel inhibition, either at rest or during exercise, does not impact the O_2 cost of contractions per se (Chen et al., 2001). Importantly, reductions in myocardial O_2 consumption with GLI are driven by the interruption of blood flow and thus a local O_2 insufficiency rather than a primary effect of mitochondrial K_{ATP} channel inhibition (Duncker et al., 2001). Based upon the evidence that PO_2mv effects were not due to changes in $\dot{V}O_2$ evaluating the mechanisms for GLI to impact $\dot{Q}O_2$ is warranted.

The administration of GLI in vivo precludes the partitioning of the effects to either the endothelial or smooth muscle cells. In the case of the endothelium it remains to be clarified

whether hyperpolarization impacts vasomotor tone via NO release or propagated hyperpolarization to the smooth muscle (conducted vasodilation). Nonetheless, the inhibition of vascular smooth muscle and endothelial K_{ATP} channels, separately or in conjunction, leads to the conclusion that the K_{ATP} channel contributes to the temporal regulation of skeletal muscle PO_2mv during contractions.

It appears unlikely that GLI-induced K_{ATP} channel inhibition in the coronary vasculature or cardiac myocytes could account for the reduced BF during exercise given that a GLI-induced decrement in cardiac output would be expected to exhibit a homogenous spatial effect on muscle blood flow and vascular conductance. In contrast to this expectation, we have demonstrated previously that the reduction of total hindlimb skeletal muscle blood flow during exercise is driven by attenuations in the muscles comprised of a primarily type I and IIa fibers (Holdsworth et al., 2015). Furthermore, these results were seen at multiple intensities of large muscle mass exercise whereas contractions in the relatively small muscle-mass spinotrapezius of healthy rats will not tax the upper limits of cardiac output. This is supported by average heart rates during spinotrapezius contractions at ~62% of the HR_{max} for sedentary Sprague-Dawley rats (Hilty et al., 1989).

We consider it unlikely that increased sympathetic nerve discharge via neuronal K_{ATP} channel inhibition would account for the reduced mean muscle PO_2mv seen herein because it has been demonstrated, in male Sprague-Dawley rats, that direct injection of GLI into the rostral ventrolateral medulla has no effect on blood pressure, HR or renal SNA (Guo et al., 2011). These findings support that GLI did not directly impact sympathetic nerve discharge in the current study and that the PO_2mv undershoot results specifically from muscle vascular K_{ATP} channel inhibition.

Conclusions

This investigation reveals a GLI-induced PO_2mv undershoot following the onset of contractions in the rat spinotrapezius, resulting in a delayed attainment of the contracting steady-state PO_2mv and reduced mean PO_2mv (evident most markedly from 30-60 s after the onset of contractions, Fig. 2A). The perturbed PO_2mv kinetics with GLI, despite the presence of redundant vasomotor control, suggests a role for the K_{ATP} channel in mobilizing the appropriate $\dot{Q}O_2$ response to maintain normal blood-myocyte O_2 driving pressure across metabolic transitions. This effect raises the question of whether muscle vascular K_{ATP} channel dysfunction underlies, in part, the $\dot{V}O_2$ kinetics limitations of clinical populations with heart failure and/or diabetes.

Table 3-1. Spinotrapezius PO_2mv parameters at rest and following the onset of contractions under control and GLI (5 mg/kg) conditions.

	Control	GLI
$PO_2mv_{(BL)}$, mmHg	34.0 ± 2.2	33.7 ± 1.6
Δ_1PO_2mv, mmHg	-10.8 ± 1.0	-12.3 ± 1.0
Δ_2PO_2mv, mmHg	1.8 ± 0.2	3.3 ± 0.7
$\Delta_{Total}PO_2mv$, mmHg	-10.5 ± 1.0	-10.4 ± 1.1
$PO_2mv_{(SS)}$, mmHg	23.6 ± 2.2	23.4 ± 1.9
TD_1, s	6.4 ± 1.0	7.2 ± 1.3
TD_2, s	69.7 ± 13.1	63.0 ± 11.5
τ_1, s	13.9 ± 1.4	16.6 ± 1.7
τ_2, s	60.4 ± 27.4	32.6 ± 7.5
MRT_1, s	20.3 ± 1.7	23.7 ± 2.2
MRT_2, s	130.1 ± 14.3	95.6 ± 8.9
MRT_{Total}	42.0 ± 14.2	79.5 ± 14.7*

Values are mean ± SE. $PO_2mv_{(BL)}$, resting PO_2mv; Δ_1PO_2mv, amplitude of the first component; Δ_2PO_2mv, amplitude of the second component; $\Delta_{Total}PO_2mv$, overall amplitude; $PO_2mv_{(SS)}$, contracting steady-state PO_2mv; TD_1, time delay of the first component; TD_2, time delay of the second component; τ_1, time constant of the first component; τ_2, time constant of the second component; MRT_1, mean response time of the first component; MRT_2, mean response time of the second component; MRT_{Total}, sum of the first and second component mean response times. One-component exponential model used for 2/12 control and 7/12 GLI. All second component parameters calculated only from two-component models (control $n = 2$, GLI $n = 7$). * $p < 0.05$ vs. control.

Figure 3-1. Spinotrapezius PO_2mv averages for 180 s post-control (open circles) and post-GLI (closed circles) infusion. The peak PO_2mv was significantly greater with GLI but not control.

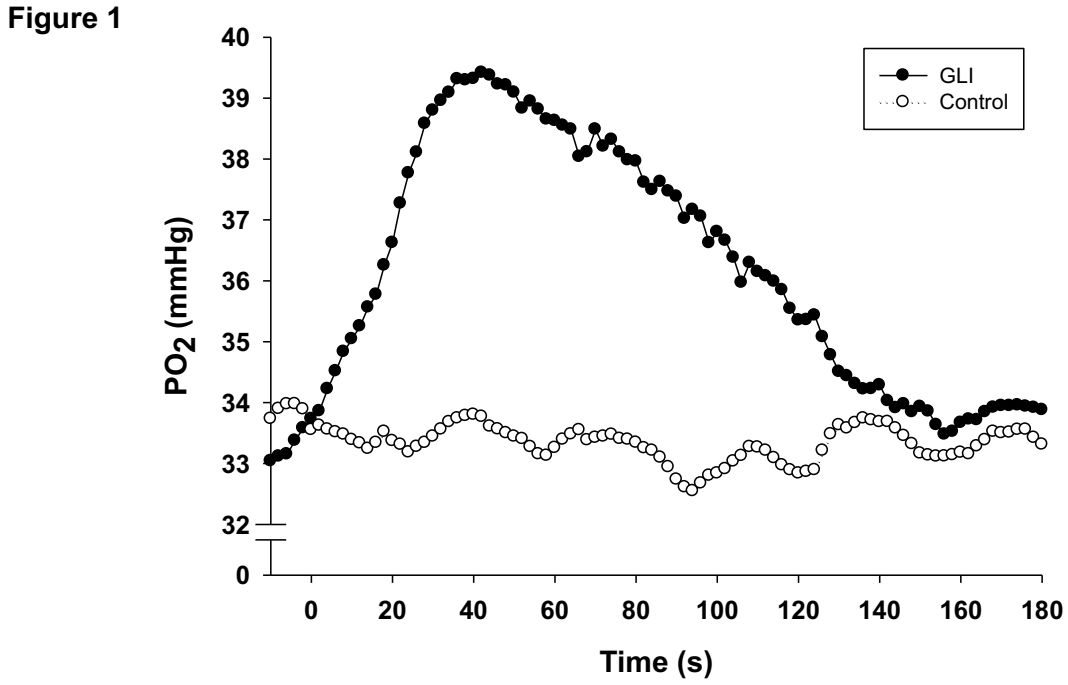

Figure 3-2. Spinotrapezius PO_2mv profiles and kinetics representations.

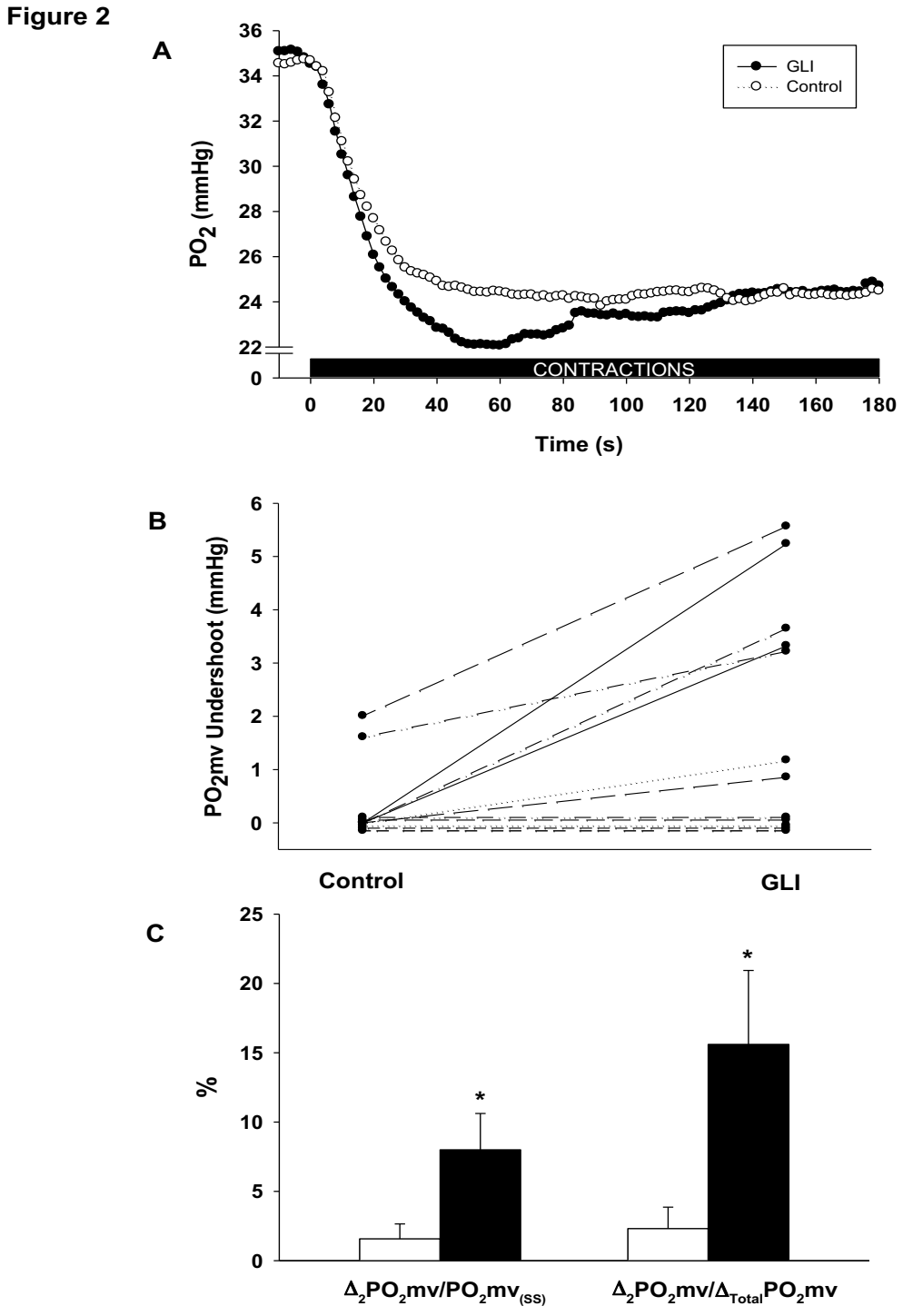

(A) Representative spinotrapezius PO_2mv profile for control (open circles) and GLI (closed circles). 180 s of contractions began at time zero. Note the divergence of PO_2mv and manifestation of the undershoot after ~20 s. (B) Individual $\Delta_2PO_2$mv (undershoot) responses to GLI. (C) The $\Delta_2PO_2$mv (undershoot) as a function of both the steady state (first grouping) and total amplitude (second grouping) * $p < 0.05$ vs control.

References

Akrouh, A., Halcomb, S.E., Nichols, C.G., Sala-Rabanal, M., 2009. Molecular biology of KATP channels and implications for health and disease. IUBMB Life 61, 971–978.

Arthur, P.G., Hogan, M.C., Bebout, D.E., Wagner, P.D., Hochachka, P.W., 1992. Modeling the effects of hypoxia on ATP turnover in exercising muscle. J. Appl. Physiol. 73, 737–742.

Bailey, J.K., Kindig, C.A., Behnke, B.J., Musch, T.I., Schmid-Schoenbein, G.W., Poole, D.C., 2000. Spinotrapezius muscle microcirculatory function: effects of surgical exteriorization. Am. J. Physiol. Heart Circ. Physiol. 279, H3131–H3137.

Banitt, P.F., Smits, P., Williams, S.B., Ganz, P., Creager, M.A., 1996. Activation of ATP-sensitive potassium channels contributes to reactive hyperemia in humans. Am. J. Physiol. 271, H1594–H1598.

Bank, A.J., Sih, R., Mullen, K., Osayamwen, M., Lee, P.C., 2000. Vascular ATP-Dependent Potassium Channels, Nitric Oxide, and Human Forearm Reactive Hyperemia. Cardiovasc. Drugs Ther. 14, 23–29.

Bauer, T.A., Reusch, J.E.B., Levi, M., Regensteiner, J.G., 2007. Skeletal muscle deoxygenation after the onset of moderate exercise suggests slowed microvascular blood flow kinetics in type 2 diabetes. Diabetes Care 30, 2880–2885.

Beech, D.J., Zhang, H., Nakao, K., Bolton, T.B., 1993. K channel activation by nucleotide diphosphates and its inhibition by glibenclamide in vascular smooth muscle cells. Br. J. Pharmacol. 110, 573–582.

Behnke, B.J., Barstow, T.J., Kindig, C.A., McDonough, P., Musch, T.I., Poole, D.C., 2002. Dynamics of oxygen uptake following exercise onset in rat skeletal muscle. Respir. Physiol. Neurobiol. 133, 229–239.

Behnke, B.J., Delp, M.D., Dougherty, P.J., Musch, T.I., Poole, D.C., 2005. Effects of aging on microvascular oxygen pressures in rat skeletal muscle. Respir. Physiol. Neurobiol. 146, 259–268.

Behnke, B.J., Kindig, C.A., Musch, T.I., Koga, S., Poole, D.C., 2001. Dynamics of microvascular oxygen pressure across the rest-exercise transition in rat skeletal muscle. Respir. Physiol. 126, 53–63.

Bijlstra, P.J., den Arend, J.A., Lutterman, J.A., Russel, F.G., Thien, T., Smits, P., 1996. Blockade of vascular ATP-sensitive potassium channels reduces the vasodilator response to ischaemia in humans. Diabetologia 39, 1562–1568.

Bodmer, S.I., Balestra, G.M., Harms, F., Johannes, T., Raat, N.J.H., Stolker, R.J., Mik, E.G., 2012. Microvascular and mitochondrial PO 2 simultaneously measured by oxygen-dependent delayed luminescence. J. Biophotonics 5, 140–151.

Chai, Y., Zhang, D.M., Lin, Y.F., 2011. Activation of cGMP-dependent protein kinase stimulates cardiac ATP-sensitive potassium channels via a ROS/calmodulin/CaMKII signaling cascade. PLoS One 6, e18191.

Chen, Y., Traverse, J.H., Zhang, J., Bache, R.J., 2001. Selective blockade of mitochondrial KATP channels does not impair myocardial oxygen consumption. Am. J. Physiol. Heart Circ. Physiol. 281, H738–H744.

Clifford, P.S., Hellsten, Y., 2004. Vasodilatory mechanisms in contracting skeletal muscle. J. Appl. Physiol. 97, 393–403.

Cole, W.C., Malcolm, T., Walsh, M.P., Light, P.E., 2000. Inhibition by protein kinase C of the K(NDP) subtype of vascular smooth muscle ATP-sensitive potassium channel. Circ. Res. 87, 112–117.

Copp, S.W., Ferreira, L.F., Herspring, K.F., Hirai, D.M., Snyder, B.S., Poole, D.C., Musch, T.I., 2009. The effects of antioxidants on microvascular oxygenation and blood flow in skeletal muscle of young rats. Exp. Physiol. 94, 961–971.

Delp, M.D., Duan, C., 1996. Composition and size of type I, IIA, IID/X, and IIB fibers and citrate synthase activity of rat muscle. J. Appl. Physiol. 80, 261–270.

Duncker, D.J., Oei, H.H., Hu, F., Stubenitsky, R., Verdouw, P.D., 2001. Role of K(ATP)(+) channels in regulation of systemic, pulmonary, and coronary vasomotor tone in exercising swine. Am. J. Physiol. Heart Circ. Physiol. 280, H22–H33.

Dunphy, I., Vinogradov, S., Wilson, D.F., 2002. Oxyphor R2 and G2: Phosphors for measuring oxygen by oxygen-dependent quenching of phosphorescence. Anal. Biochem. 310, 191–198.

Farouque, H.M.O., Meredith, I.T., 2003. Effects of inhibition of ATP-sensitive potassium channels on metabolic vasodilation in the human forearm. Clin. Sci. (Lond). 104, 39–46.

Ferreira, L.F., Hageman, K.S., Hahn, S., Williams, J., Padilla, D.J., Poole, D.C., Musch, T.I., 2006a. Muscle microvascular oxygenation in chronic heart failure: role of nitric oxide availability. Acta Physiol. (Oxf). 188, 3–13.

Ferreira, L.F., Padilla, D.J., Williams, J., Hageman, K.S., Musch, T.I., Poole, D.C., 2006b. Effects of altered nitric oxide availability on rat muscle microvascular oxygenation during contractions. Acta Physiol. (Oxf). 186, 223–232.

Ferreira, L.F., Poole, D.C., Barstow, T.J., 2005. Muscle blood flow-O2 uptake interaction and their relation to on-exercise dynamics of O2 exchange. Respir. Physiol. Neurobiol. 147, 91–103.

George, S., McBurney, A., Cole, A., 1990. Possible protein binding displacement interaction between glibenclamide and metolazone. Eur. J. Clin. Pharmacol. 38, 93–95.

Grassi, B., Rossiter, H.B., Zoladz, J.A., 2015. Skeletal Muscle Fatigue and Decreased Efficiency: Two Sides of the Same Coin? Exerc. Sport Sci. Rev. 43, 75–83.

Guo, Q., Jin, S., Wang, X.L., Wang, R., Xiao, L., He, R., Wu, Y., 2011. Hydrogen sulfide in the rostral ventrolateral medulla inhibits sympathetic vasomotor tone through ATP-sensitive K+ channels. J. Pharmacol. Exp. Ther. 338, 458–465.

Heinonen, I., Koga, S., Kalliokoski, K.K., Musch, T.I., Poole, D.C., 2015. Heterogeneity of Muscle Blood Flow and Metabolism: Influence of Exercise, Aging and Disease States. Exerc. Sport Sci. Rev. 43, 117-124.

Herspring, K.F., Ferreira, L.F., Copp, S.W., Snyder, B.S., Poole, D.C., Musch, T.I., 2008. Effects of antioxidants on contracting spinotrapezius muscle microvascular oxygenation and blood flow in aged rats. J. Appl. Physiol. 105, 1889–1896.

Hilty, M.R., Groth, H., Moore, R.L., Musch, T.I., 1989. Determinants of VO2max in rats after high-intensity sprint training. J. Appl. Physiol. 66, 195–201.

Hirai, D.M., Copp, S.W., Ferguson, S.K., Holdsworth, C.T., Musch, T.I., Poole, D.C., 2013. The NO donor sodium nitroprusside: evaluation of skeletal muscle vascular and metabolic dysfunction. Microvasc. Res. 85, 104–111.

Hogan, M.C., Arthur, P.G., Bebout, D.E., Hochachka, P.W., Wagner, P.D., 1992. Role of O2 in regulating tissue respiration in dog muscle working in situ. J. Appl. Physiol. 73, 728–736.

Holdsworth, C.T., Copp, S.W., Ferguson, S.K., Sims, G.E., Poole, D.C., Musch, T.I., 2015. Acute blockade of ATP-sensitive K+ channels impairs skeletal muscle vascular control in rats during treadmill exercise. Am. J. Physiol. Heart Circ. Physiol. 11, H1434-H1442.

Joyner, M.J., Casey, D.P., 2015. Regulation of Increased Blood Flow (Hyperemia) to Muscles During Exercise: A Hierarchy of Competing Physiological Needs. Physiol. Rev. 95, 549–601.

Kawano, T., Zoga, V., Kimura, M., Liang, M.Y., Wu, H.E., Gemes, G., McCallum, J.B., Kwok, W.M., Hogan, Q.H., Sarantopoulos, C.D., 2009. Nitric oxide activates ATP-sensitive potassium channels in mammalian sensory neurons: action by direct S-nitrosylation. Mol. Pain 5, 12.

Keller, D.M., Ogoh, S., Greene, S., Olivencia-Yurvati, A., Raven, P.B., 2004. Inhibition of KATP channel activity augments baroreflex-mediated vasoconstriction in exercising human skeletal muscle. J. Physiol. 561, 273–282.

Krogh, A., Lindhard, J., 1913. The regulation of respiration and circulation during the initial stages of muscular work. J. Physiol. 47, 112–36.

Kubo, M., Nakaya, Y., Matsuoka, S., Saito, K., Kuroda, Y., 1994. Atrial natriuretic factor and isosorbide dinitrate modulate the gating of ATP-sensitive K+ channels in cultured vascular smooth muscle cells. Circ. Res. 74, 471–476.

Larsen, J.J., Dela, F., Madsbad, S., Vibe-Petersen, J., Galbo, H., 1999. Interaction of sulfonylureas and exercise on glucose homeostasis in type 2 diabetic patients. Diabetes Care 22, 1647–1654.

Murphy, M.E., Brayden, J.E., 1995. Nitric oxide hyperpolarizes rabbit mesenteric arteries via ATP-sensitive potassium channels. J. Physiol. 486 Pt 1, 47–58.

Nakai, T., Ichihara, K., 1994. Effects of diazoxide on norepinephrine-induced vasocontraction and ischemic myocardium in rats. Biol. Pharm. Bull. 17, 1341–1344.

O'Connor, E., Green, S., Kiely, C., O'Shea, D., Egaña, M., 2015. Differential effects of age and type 2 diabetes on dynamic vs. peak response of pulmonary oxygen uptake during exercise. J. Appl. Physiol. 118, 1031–1039.

Padilla, D.J., McDonough, P., Behnke, B.J., Kano, Y., Hageman, K.S., Musch, T.I., Poole, D.C., 2007. Effects of Type II diabetes on muscle microvascular oxygen pressures. Respir. Physiol. Neurobiol. 156, 187–195.

Piepoli, M.F., Guazzi, M., Boriani, G., Cicoira, M., Corrà, U., Dalla Libera, L., Emdin, M., Mele, D., Passino, C., Vescovo, G., Vigorito, C., Villani, G., Agostoni, P., 2010a. Exercise intolerance in chronic heart failure: mechanisms and therapies. Part II. Eur. J. Cardiovasc. Prev. Rehabil. 17, 643–648.

Piepoli, M.F., Guazzi, M., Boriani, G., Cicoira, M., Corrà, U., Dalla Libera, L., Emdin, M., Mele, D., Passino, C., Vescovo, G., Vigorito, C., Villani, G.Q., Agostoni, P., 2010b. Exercise intolerance in chronic heart failure: mechanisms and therapies. Part I. Eur. J. Cardiovasc. Prev. Rehabil. 17, 637–642.

Poole, D.C., Behnke, B.J., McDonough, P., McAllister, R.M., Wilson, D.F., 2004. Measurement of muscle microvascular oxygen pressures: compartmentalization of phosphorescent probe. Microcirculation 11, 317–326.

Poole, D.C., Hirai, D.M., Copp, S.W., Musch, T.I., 2012. Muscle oxygen transport and utilization in heart failure: implications for exercise (in)tolerance. Am. J. Physiol. Heart Circ. Physiol. 302, H1050–H1063.

Poole, D.C., Jones, A.M., 2012. Oxygen uptake kinetics. Compr. Physiol. 2, 933–996.

Regensteiner, J.G., Bauer, T.A., Reusch, J.E., Brandenburg, S.L., Sippel, J.M., Vogelsong, A.M., Smith, S., Wolfel, E.E., Eckel, R.H., Hiatt, W.R., 1998. Abnormal oxygen uptake kinetic responses in women with type II diabetes mellitus. J. Appl. Physiol. 85, 310–317.

Richardson, R.S., Noyszewski, E.A., Kendrick, K.F., Leigh, J.S., Wagner, P.D., 1995. Myoglobin O2 desaturation during exercise. Evidence of limited O2 transport. J. Clin. Invest. 96, 1916–1926.

Rumsey, W.L., Vanderkooi, J.M., Wilson, D.F., 1988. Imaging of phosphorescence: a novel method for measuring oxygen distribution in perfused tissue. Science 241, 1649–1651.

Sacre, J.W., Jellis, C.L., Haluska, B.A., Jenkins, C., Coombes, J.S., Marwick, T.H., Keske, M.A., 2015. Association of Exercise Intolerance in Type 2 Diabetes With Skeletal Muscle Blood Flow Reserve. JACC. Cardiovasc. Imaging 8, 913–21.

Sadraei, H., Beech, D.J., 1995. Ionic currents and inhibitory effects of glibenclamide in seminal vesicle smooth muscle cells. Br. J. Pharmacol. 115, 1447–1454.

Schrage, W.G., Dietz, N.M., Joyner, M.J., 2006. Effects of combined inhibition of ATP-sensitive potassium channels, nitric oxide, and prostaglandins on hyperemia during moderate exercise. J. Appl. Physiol. 100, 1506–1512.

Silva, K.E., Barbosa, H.C., Rafacho, A., Bosqueiro, J.R., Stoppiglia, L.F., Carneiro, E.M., Borelli, M.I., Del Zotto, H., Gagliardino, J.J., Boschero, A.C., 2008. INGAP-PP up-regulates the expression of genes and proteins related to K+ATP channels and ameliorates Ca2+ handling in cultured adult rat islets. Regul. Pept. 148, 39–45.

Tateishi, J., Faber, J.E., 1995. ATP-Sensitive K+ Channels Mediate 2D-Adrenergic Receptor Contraction of Arteriolar Smooth Muscle and Reversal of Contraction by Hypoxia. Circ. Res. 76, 53–63.

Thomas, G.D., Hansen, J., Victor, R.G., 1997. Atp-sensitive potassium channels mediate contraction- induced attenuation of sympathetic vasoconstriction in rat skeletal muscle. J. Clin. Invest. 99, 2602–2609.

Wilson, D.F., Erecińska, M., Drown, C., Silver, I.A., 1977. Effect of oxygen tension on cellular energetics. Am. J. Physiol. 233, C135–140.

Yoshida, T., Inoue, R., Morii, T., Takahashi, N., Yamamoto, S., Hara, Y., Tominaga, M., Shimizu, S., Sato, Y., Mori, Y., 2006. Nitric oxide activates TRP channels by cysteine S-nitrosylation. Nat. Chem. Biol. 2, 596–607.

Chapter 4 - Vascular K_{ATP} channels reduce severe muscle O_2-delivery to O_2-utilization mismatch during contractions in chronic heart failure rats

Abstract

The vascular ATP-sensitive K^+ (K_{ATP}) channel is a mediator of skeletal muscle microvascular O_2 delivery (PO_2mv) during contractions. The objective was to test the hypothesis that K_{ATP} channel inhibition would augment the PO_2mv undershoot, increase the time to reach the steady-state PO_2mv and decrease the mean PO_2mv during contractions of the spinotrapezius muscle in chronic heart failure rats. Muscle PO_2mv (phosphorescence quenching) was measured during 180 s of 1-Hz twitch contractions (~6 V) under control, glibenclamide (5 mg/kg) and pinacidil (PIN; 5 mg/kg) conditions in 16 Sprague-Dawley rats with heart failure induced via myocardial infarction (coronary artery ligation). Glibenclamide increased the undershoot (control: 2.3 ± 0.4, GLI: 4.1 ± 0.5 mmHg, $p < 0.05$), reduced baseline (control: 28.3 ± 0.9, GLI: 24.8 ± 1.0 mmHg $p < 0.05$) and mean PO_2mv (control: 20.6 ± 0.6, GLI: 17.6 ± 0.3 mmHg, $p < 0.05$), and slowed the attainment of steady-state PO_2mv. PIN reversed the effects of GLI on the baseline PO_2mv, undershoot, mean PO_2mv and time to reach the steady state PO_2mv ($p < 0.05$ for all). Inhibition of K_{ATP} channels exacerbates the transient mismatch of O_2-delivery to O_2-utilization in heart failure rats and can be reversed by PIN. These data suggest that the muscle hypoxia in heart failure augments the role of K_{ATP} channels in attenuating the decrease in muscle O_2-delivery to O_2-utilization matching at the onset of contractions.

Introduction

Oxygen transfer to peripheral tissues via both convective and diffusive routes is routinely interrupted as part of the inexorable progression of chronic, congestive heart failure (rev. by Poole et al., 2012). A growing, but likely incomplete list of this dysfunction now includes decrements in skeletal muscle blood flow and vascular conductance, lowering of the muscle microvascular O_2 pressure (PO_2mv), and derangement of capillary structure, geometry and hemodynamics (rev. by Piepoli et al., 2010a, 2010b). As a result of these effects, inadequate tissue O_2 transport during the tremendous metabolic challenge imposed by exercise contributes to reductions in work capacity that are commensurate with the severity of heart failure (Miyazaki et al., 2007; Piepoli et al., 2010a, 2010b). For investigators interested in evaluating the dysfunction of cardiopulmonary control in general, and peripheral vascular control specifically, direct measurement of muscle PO_2mv provides excellent insight because it represents the final pressure head responsible for blood-myocyte O_2 diffusion. More importantly, because PO_2mv is set by the ratio of O_2-delivery to O_2-utilization, and occurs at the terminal cell-to-cell interface of the O_2 transport chain, it is impacted by upstream cardiopulmonary perturbations. This makes the PO_2mv sensitive to both the spatial and temporal aspects of vascular function and accordingly it has been exploited in investigations of heart failure (Diederich et al., 2002) and nitric oxide (NO) function (Ferreira et al., 2006b).

Maintaining adequate muscle PO_2mv by tightly matching O_2-supply to O_2-demand is crucial given that even transient mismatch can cause a premature decline in muscle PCr stores and the accumulation of muscle metabolites associated with fatigue such as ADP, H^+, K^+ and P_i (Hogan et al., 1992; Richardson et al., 1995; Wilson et al., 1977). A potassium channel with sensitivity to ATP and ADP (K_{ATP}) suggests a potential transducer between tissue metabolism

and cell membrane potential via K^+ efflux-induced hyperpolarization. A channel with these properties in vascular smooth muscle cells presents a unique mechanism for coupling vascular tone, and thus O_2 availability, directly to skeletal muscle metabolism. It is readily evident that the K_{ATP} channel can function this way *in vivo* as inhibition exaggerates baroreflex-mediated vasoconstriction (Keller et al., 2004) and activation attenuates α-adrenergic vasoconstriction (Nakai and Ichihara, 1994; Tateishi and Faber, 1995). It remains unclear, however, under which circumstances the channel is obligatory to adequate skeletal muscle O_2 transport. Individual studies of K_{ATP} channel inhibition are equivocal; some demonstrating robust effects on the magnitude of the hyperemic response at steady-state (Banitt et al., 1996; Bank et al., 2000; Bijlstra et al., 1996; Holdsworth et al., 2015) while others find no change (Duncker et al., 2001; Farouque and Meredith, 2003; Schrage et al., 2006). However, properties of the local micro-environment are crucial to the role of the channel in vivo and will differ between species, disease states and events of cell stress (e.g. exercise) . In particular, K_{ATP} channel function is likely a requisite response to ischemia and thus cell hypoxia (Bijlstra et al., 1996; Nakai and Ichihara, 1994; Suzuki et al., 2002; Tateishi and Faber, 1995; Wheaton and Chandel, 2011). Relative to healthy individuals these are primary attributes of muscle tissue in heart failure as discussed above. Therefore, the purpose of the study was to test the hypothesis that inhibition of vascular K_{ATP} channels via glibenclamide (GLI) would increase both the magnitude of the PO_2mv undershoot and overall time to reach the contracting steady-state PO_2mv in the spinotrapezius muscle of heart failure rats. Additionally, it was anticipated that these perturbations would drive a reduction in the mean PO_2mv during the transition to steady-state PO_2mv and that the effects of GLI would be reversed by the K_{ATP} channel activator pinacidil (PIN).

Methods

Ethical approval

All procedures were approved by the Institutional Animal Care and Use Committee of Kansas State University under the guidelines established by the National Institutes of Health. 16 adult male Sprague-Dawley rats (3-6 months old) were maintained in accredited animal facilities (Association for the Assessment and Accreditation of Laboratory Animal Care) at Kansas State University on a 12-h light/12-h dark cycle with food and water provided *ad libitum*.

Myocardial infarction procedures

All rats underwent induction of a myocardial infarction (MI) via ligation of the left main coronary artery which has been shown to result reliably in the development of chronic, congestive heart failure (Musch and Terrell, 1992). Briefly, each rat (~275 g) was anesthetized with a gas mixture of 5% isoflurane-O_2 and intubated for mechanical ventilation on a rodent respirator (model 680, Harvard Instruments, Holliston, USA) with subsequent maintenance on a 3% isoflurane-O_2 gas mixture for the duration of the procedure. A left thoracotomy was performed to expose the heart through the fifth intercostal space. Exteriorization of the heart provided access to the left main coronary artery which was ligated with a 6-0 silk suture ~1-2 mm distal to the edge of the left atrium. The muscles of the thorax were then closed with 4-0 gut, and the skin incision was closed with 3-0 silk followed by an administration of the analgesic agents bupivacaine (1.5 $mg \cdot kg^{-1}$ subcutaneously) and buprenorphine (0.01–0.05 $mg \cdot kg^{-1}$ i.m.) as well as ampicillin (50 $mg \cdot kg^{-1}$ i.m.) to reduce the risk of infection. Upon removal from mechanical ventilation and withdrawal of anesthesia the rats were monitored ~8-12 h post-operatively for the development of arrhythmias and undue stress with care administered as needed. The recovery duration prior to the final, PO_2mv protocol was ≥21 days which is

consistent with the time course for complete remodeling of necrotic myocardial tissue (Fishbein et al., 1978). During this time the rats were monitored daily (appetite, weight loss, gait/posture, etc.) in conjunction with the university veterinary staff.

Surgical instrumentation

On the day of the final protocol the rats were anesthetized initially with a 5% isoflurane-O_2 mixture and maintained on a 3% isoflurane-O_2 mixture for the duration of the surgical instrumentation. The carotid artery was cannulated and a two-French-catheter-tipped pressure transducer (Millar Instruments, Houston, USA) was advanced into the left ventricle (LV) for the measurement of left ventricular end diastolic pressure (LVEDP). Subsequently, cannulation of both the carotid and caudal arteries was performed with PE-10 connected to PE-50 (Intra-Medic polyethylene tubing, Clay Adams, Spark, USA) for the measurement of mean arterial pressure (MAP) and heart rate (HR) as well as infusion of the phosphorescent probe G2 (carotid) and for blood sampling and administration of anesthetics (caudal). Isoflurane-O_2 inhalation was progressively removed as anesthesia was maintained with pentobarbital sodium administered via the caudal artery catheter to effect. Depth of anesthesia was monitored at frequent and regular intervals via the blink and toe-pinch reflexes as well as magnitude and frequency of ventilation. Access to the spinotrapezius was achieved by surgically reflecting the overlying skin and fascia. The spinotrapezius muscle was selected because the fiber-type composition and oxidative capacity closely resembles that of the human quadriceps muscle group which makes it a useful analog of human locomotor muscle (Delp and Duan, 1996). During both the surgical preparation and experimental protocol the muscle was superfused frequently with Krebs-Hensleit bicarbonate-buffered solution consisting of (in mM) 4.7 KCl, 2.0 $CaCl_2$, 2.4 $MgSO_4$, 131 NaCl, and 22 $NaHCO_3$ equilibrated with 5% CO_2 and 95% N_2 (pH 7.4, 37-38°C). Exposed tissue

surrounding the spinotrapezius muscle was covered with Saran wrap (Dow Brands, Indianapolis, IN) to reduce dehydration and limit the exposure of GLI and PIN to the spinotrapezius. Stainless steel electrodes were sutured to the rostral (cathode) and caudal (anode) regions of the spinotrapezius muscle for electrically-induced twitch contractions. As previously reported by our laboratory these surgical procedures do not impact the microvascular integrity and responsiveness of the rat spinotrapezius muscle (Bailey et al., 2000).

Drugs

The pharmacological sulphonylurea derivative GLI (494 g mol^{-1}; 5-chloro-*N*-(4-[*N*-(cyclohexylcarbamoyl)sulfamoyl]phenethyl)-2-methoxybenzamide; Sigma-Aldrich, St Louis, MO, USA) was used to inhibit vascular K_{ATP} channels. Given that GLI is difficult to maintain in solution, 25 mg of GLI was dissolved in 99:1 ratio of distilled water/NaOH (1 M) during continuous sonication to produce a 2.5 mg ml^{-1} stock solution. A 5 mg kg^{-1} dose was drawn from the stock solution and diluted to ~3 ml with Krebs-Hensleit solution. It has been reported previously that GLI is a selective K_{ATP} channel blocker at concentrations below 5 μmol L^{-1} (Beech et al., 1993; Sadraei and Beech, 1995). The current dose of 5 mg kg^{-1} for rats of a mean body mass of 463 g equates to a blood concentration of ~140 μmol L^{-1}. Given that 98-99% of GLI is bound to plasma protein, the effective blood concentration of GLI is ~2-3 μmol L^{-1} (George et al., 1990) which is in the range for GLI to be selective for K_{ATP} channels without inhibition of Ca^{+} channel current (Sadraei and Beech, 1995). This dosing strategy, based on smooth muscle cell investigations, was shown to elicit a degree of K_{ATP} channel blockade for swine in vivo (Duncker et al., 2001). See Discussion for further considerations of K_{ATP} channel inhibition. PIN (245 g mol^{-1},N-cyano-N'-pyridin-4-yl-N''-(1,2,2-trimethylpropyl)guanidine; Sigma-Aldrich, St Louis, MO, USA) is readily dissolved in distilled water and was diluted to ~3

ml with Krebs-Hensleit solution before being administered to reverse vascular K_{ATP} channel inhibition at the same dose as GLI.

Experimental protocol

Three separate contraction bouts were performed under control (vehicle), GLI (5 mg/kg) and PIN (5 mg/kg) conditions. The vehicle was administered for control via superfusion (3 ml) of the spinotrapezius during 180 s of continuous PO_2mv recording. The recording was extended for an additional 90-180 s to ensure that baseline PO_2mv had stabilized at which time muscle contraction was evoked via electrical stimulation (1 Hz, ~6 V, 2-ms pulse duration, model s48; Grass Technologies, Quincy, MA) for 180 s. This protocol has been shown to increase blood flow four- to five-fold and metabolic rate six- to seven-fold without altering blood pH and is consistent with moderate intensity exercise (Behnke et al., 2002; Hirai et al., 2013). Immediately upon cessation of electrical stimulation an arterial blood sample was drawn (~0.8 ml) for the determination of blood gases, hematocrit, pH, [lactate] and [glucose]. After a ~25 min recovery the second contraction bout was performed in an identical fashion to the first after the administration of GLI (5 mg/kg). This was repeated for the third contraction bout with the administration of PIN. As previously reported by our laboratory, >20 min recovery elicits reproducible PO_2mv responses (Copp et al., 2009; Herspring et al., 2008). At the end of the protocol, rats were euthanized with intra-arterial pentobarbital sodium overdose (>50 mg/kg) and subsequent removal of the heart. The lungs, right ventricle (RV), LV and atria were separated and weighed. Measurement of infarct size in the LV was made via planimetry as described previously (Ferreira et al., 2006a).

Spinotrapezius PO_2mv measurement

PO_2mv was measured via phosphorescence quenching using a frequency domain phosphorometer (PMOD 5000; Oxygen Enterprises, Philadelphia, PA). As described previously (Behnke et al., 2001), this technique applies the Stern-Volmer relationship (Rumsey et al., 1988), which describes the quantitative O_2 dependence of the phosphorescent probe G2 via the equation:

$$PO_2mv = [(\tau°/\tau) - 1]/(k_Q \cdot \tau°)$$

where k_Q is the quenching constant and τ and $\tau°$ are the phosphorescence lifetimes at the ambient O_2 concentration and in the absence of O_2, respectively. For the phosphorescent probe G2, k_Q is 273 $mmHg^{-1}$ s^{-1} and $\tau°$ is 251 μs (Bodmer et al., 2012; Dunphy et al., 2002). These characteristics do not change over the physiological range of pH (~7.4) and temperature (~38°C) *in vivo* and, therefore, the phosphorescence lifetime is affected solely by the O_2 partial pressure. The Pd-porphyrin cores of phosphor probes bind to albumin; the primary macromolecule in plasma. This quality as well as the probes' negative charge ensures restriction to the vascular compartment, of which, the capillary bed volumetrically constitutes the major intramuscular space (Poole et al., 2004). After infusion of G2 the common end of the bifurcated light guide with a >500 μm penetration depth was positioned ~2-4 mm superficial to the dorsal surface of the exposed spinotrapezius muscle in an area devoid of macro-vessels. The phosphorometer modulates sinusoidal excitation frequencies between 100 Hz and 20 kHz and allows phosphorescence lifetime measurements from 10 μs to ~2.5 ms. PO_2mv was measured continuously and recorded at 2-s intervals throughout the duration of the experimental protocol.

Analysis of spinotrapezius PO_2mv kinetics

PO_2mv time course was determined via exponential regression analysis by applying the Levenberg-Marquardt algorithm (SigmaPlot 11.0; Systat software, San Jose, CA) to the contraction-induced PO_2mv transient. The sum of squared residuals was used to indicate the appropriateness of the model fit. PO_2mv responses were fit with either a one- or two-component model as follows.

One component:

$$PO_2mv_{(t)} = PO_2mv_{(BL)} - \Delta PO_2mv\ (1 - e^{-(t - TD)/\tau})$$

Two component:

$$PO_2mv_{(t)} = PO_2mv_{(BL)} - \Delta_1 PO_2mv\ (1 - e^{-(t - TD_1)/\tau_1}) + \Delta_2 PO_2mv\ (1 - e^{-(t - TD_2)/\tau_2})$$

$PO_2mv_{(t)}$ is the PO_2mv at a given time *t*; $PO_2mv_{(BL)}$ corresponds to the pre-contracting resting PO_2mv; Δ_1 and Δ_2 are the amplitudes for the first and second components, respectively; TD_1 and TD_2 are the independent time delays for each component; and τ_1 and τ_2 are the time constants (i.e. time to 63% of the response) for each component. Goodness of fit was determined using three criteria: the coefficient of determination, sum of squared residuals, and visual inspection (Behnke et al., 2002).

The mean response time (MRT_1) was used to describe the overall dynamics of the PO_2mv fall following the onset of muscle contractions via the equation:

$$MRT_1 = TD_1 + \tau_1$$

The MRT_1 analysis was limited to the first component of the PO_2mv response given that inclusion of an emergent second component underestimates the speed of the PO_2mv fall at the onset of contractions. In the event of a second component the MRT_2 was calculated using the following equation:

$MRT_2 = TD_2 + \tau_2$

To determine the overall time taken to reach the steady-state PO_2mv the $MRT_{(Total)}$ was calculated via the equation:

$MRT_{Total} = MRT_1 + MRT_2$

The $MRT_{(Total)}$ does not equal the sum of the MRT_1 and MRT_2 averages because MRT_2 is independent of the calculation of $MRT_{(Total)}$. The purpose of the second component kinetics parameters is to represent the speed with which the $PO_2mv_{(SS)}$ is reached after the initial fall in PO_2mv. For this reason, the MRT_2 averages are calculated from rats with a two-component fit only. However, the calculation of $MRT_{(Total)}$ necessarily reflects the absence of MRT_2 (i.e. effectively zero) for rats fit with a one-component model.

Mean PO_2mv was calculated as the average PO_2mv from the contractions onset through the duration of $MRT_{(Total)}$.

Results

The final body weight for all CHF rats was 463 ± 12 g. Table 1 summarizes the descriptive statistics for the central indices of CHF. Arterial blood [lactate], [glucose], PO_2, PCO_2, O_2 saturation, hematocrit and pH were not different with GLI relative to control and were not different after reversal of K_{ATP} channel inhibition with PIN ($p > 0.05$ for all). The MAP (control: 110 ± 4, GLI: 114 ± 5, $p > 0.05$) and HR (control: 326 ± 10, GLI: 337 ± 14, $p > 0.05$) at the start of contractions with GLI was not different from control. PIN reduced MAP at the start of contractions compared to GLI (PIN: 100 ± 6, GLI: 114 ± 5 mmHg, $p < 0.05$), but did not change HR (PIN: 367 ± 14, GLI: 337 ± 14 mmHg, $p > 0.05$).

The kinetics parameters are provided comprehensively in Table 2. During the control condition 11 of 16 rats exhibited PO_2mv profiles that transiently fell below the contracting steady-state (termed an "undershoot", $\Delta_2PO_2$mv) necessitating a two-component model fit. Conversely, during GLI the two-component model was required for 15 of 16 rats and during PIN for 11 of 12 rats. The goodness of fit for the models was demonstrated by the excellent r^2 (0.97 ± 0.005) and the sum of squared residuals (18.9 ± 3.0). Compared to control, GLI reduced the PO_2mv baseline (CON: 28.3 ± 0.9, GLI: 24.8 ± 1.0 mmHg $p < 0.05$) and the amplitude of the the initial fall in PO_2mv ($\Delta_1PO_2$mv). However, the amplitude as a function of the reduced baseline PO_2mv was not different (control: 39 ± 2, GLI: 39 ± 2 %, $p > 0.05$). GLI increased the undershoot of the contracting steady-state (control: 2.3 ± 0.4, GLI: 4.1 ± 0.5 mmHg, $p < 0.05$), but there was no difference in the speed of the fall in PO_2mv at the onset of contractions as indicated by the time delay, time constant and mean response time of the first component (τ_1, TD_1, and MRT_1, respectively; $p > 0.05$ for all). GLI slowed the attainment of the steady state as indicated by an increase in the time constant and mean response time of the second component and total mean

response time (τ_2, MRT_2, and $MRT_{(Total)}$ respectively). The mean PO_2mv (control: 20.6 ± 0.6, GLI: 17.6 ± 0.3 mmHg, $p < 0.05$) over the contraction transient was also reduced with GLI.

Compared to GLI, PIN increased the $PO_2mv_{(BL)}$ and $PO_2mv_{(SS)}$ with no difference in the Δ_1PO_2mv. PIN decreased the TD_1, but did not change either the τ_1 or MRT_1 during the initial fall in PO_2mv compared to GLI. PIN sped the attainment of the steady state by reducing the Δ_2PO_2mv and thus $MRT_{(Total)}$ compared to GLI. The mean PO_2mv (GLI: 17.6 ± 0.3, PIN: 25.7 ± 0.5 mmHg, $p < 0.05$) over the contraction transient was increased compared to GLI.

Given that PIN could not be compared to control all results were compared between conditions with paired Student's *t*-tests on the basis of the *a priori* hypotheses. The level of significance was set at $p < 0.05$. Results are presented as means ± SE.

Discussion

K_{ATP} channel inhibition via GLI resulted in extensive perturbations of the spinotrapezius PO_2mv profile at the onset of contractions in heart failure rats. The major effects of GLI were 1) a reduction in the baseline PO_2mv 2) a near doubling of the PO_2mv undershoot and 42% increase in the overall time to reach the contracting steady-state and 3) a reduced mean PO_2mv during the transition from contraction onset to the steady-state PO_2mv. GLI caused the PO_2mv to undershoot the contracting steady-state by a remarkable ~60% of net amplitude compared to ~20% in the control. Crucially, the mismatch of O_2-delivery to O_2-utilization coincides with the rapid phase II increase in $\dot{V}O_2$ kinetics (Behnke et al., 2002). Exacerbating the fall in skeletal muscle PO_2mv due to a sluggish increase in $\dot{Q}O_2$ is likely to impact cellular metabolism and may contribute to the slowing of $\dot{V}O_2$ kinetics in heart failure patients (Ferreira et al., 2005; Wheaton and Chandel, 2011; Wilson et al., 1977). These data suggest that vascular smooth muscle and/or endothelial K_{ATP} channel function are fundamental to the control of muscle PO_2mv kinetics at the onset of contractions in heart failure, and the K_{ATP} channel may represent one of the few well-preserved mechanisms of skeletal muscle vascular control in heart failure. The K_{ATP} channel-induced protection against severe O_2-delivery to O_2-utilization mismatch during contractions raises serious concern when sulphonylureas such as GLI are prescribed for patients with coincident diabetes and heart failure.

The central indices of dysfunction (Table 1) suggests that the severity of heart failure was moderate in these animals (Ferreira et al., 2006a). The spectrum included animals with LVEDP's above 30 mmHg and MI size's greater than 40% (severe heart failure) however the sample size was not sufficient for adequately powered statistical comparisons. Moderate heart failure induced via the rat model of coronary artery ligation results in decrements to skeletal muscle blood flow,

vascular conductance, PO_2mv kinetics, VO_2max, and time-to-exhaustion during exercise. However, the moderate heart failure herein may underestimate the effect of GLI on the PO_2mv profiles during contractions.

K_{ATP} channel manipulation of the steady-state $\dot{Q}O_2$ has been characterized previously for in vivo electrical stimulation (Thomas et al., 1997), reactive hyperemia (Banitt et al., 1996; Bank et al., 2000; Bijlstra et al., 1996) and exercise-induced hyperemia (Holdsworth et al., 2015). Our laboratory has also demonstrated that GLI increased the prevalence of the undershoot and prolonged the time to reach the contracting steady-state PO_2mv in the spinotrapezius of healthy rats (Holdsworth, pending). Conversely, the available evidence *in vivo* suggests that there is no change in $\dot{V}O_2$ during whole body exercise (Larsen et al., 1999) with GLI and that mitochondrial K_{ATP} channel inhibition does not impact the O_2 cost of contractions (Chen et al., 2001). These data indicate that it is appropriate to interpret GLI-induced changes in $\dot{Q}O_2$ as the primary driver of the perturbed PO_2mv profile.

The small-muscle mass preparation poses an advantage for investigations of peripheral vascular control because it does not tax the limits of cardiac output. This is fortunate for an investigation of K_{ATP} channel function in heart failure because the channel has a role in cardiac function. In heart failure rats it appears that the vascular K_{ATP} channel pathway remains intact given the marked sensitivity of the PO_2mv profile to both GLI and PIN. The PO_2mv profiles of the heart failure rats herein exhibit the characteristic undershoot demonstrated previously by our laboratory (Behnke et al., 2001; Hirai et al., 2014) and permitted the statistical comparison of second-component kinetics between control and GLI which has not been possible previously. It was revealed that the magnitude of the PO_2mv undershoot was increased and the intrinsic speed of the second component, independent of the undershoot, was slowed by GLI. Mean PO_2mv was

also lower across the metabolic transition and, in contrast to previous results in healthy rats, the baseline PO_2mv was reduced with GLI. Our findings also extend upon previous investigations by demonstrating reversal of the major effects of GLI via PIN. The robust role of vascular K_{ATP} channels in heart failure is not surprising given the shift in metabolic phenotype towards a greater reliance on glycolytic pathways (Delp et al., 1997) and thus increased intracellular [ADP] (Hogan et al., 1992; Wilson et al., 1977). In addition, the loss of vasodilatory redundancy in heart failure (e.g. NO-bioavailability) is likely to increase reliance on the intact K_{ATP} channel pathway and these data are the first evidence to support the argument that the role of the K_{ATP} channel in vascular control can be masked by the ample hyperemic reserve in healthy conditions.

GLI clearly exaggerates many of the heart-failure induced perturbations of skeletal muscle PO_2mv kinetics including the PO_2mv undershoot and prolonged recovery to the final contracting steady-state PO_2mv (Ferreira et al., 2006a). This effect is also well-characterized in other O_2 supply-limited conditions such as aging (Behnke et al., 2005) and diabetes (Padilla et al., 2007) which are often coincident conditions for heart failure patients. The exacerbation of this dysregulation with GLI is physiologically relevant given that these populations present with severe exercise intolerance (Piepoli et al., 2010a, 2010b; Sacre et al., 2015) due, in part, to inadequate regulation of the skeletal muscle PO_2mv pressure head (rev. by Poole et al., 2012). Both the magnitude and timing (i.e. during the exponential rise in $\dot{V}O_2$) of the decrements in PO_2mv also indicates that the perturbations of [metabolite] are likely to impair muscle work capacity and/or $\dot{V}O_2$ kinetics.

The PO_2mv undershoot has been attributed, in part, to reductions in NO-bioavailability (Ferreira et al., 2006a, 2006b) and the results herein indicate that the K_{ATP} channel protects against a severe mismatch of O_2-delivery to O_2-utilization. The shared contribution of attenuated

NO and K_{ATP} channel-mediated $\dot{Q}O_2$ to the PO_2mv undershoot suggests that these pathways are not merely independent, parallel mechanisms, but rather synergistic mediators of O_2-delivery to O_2-utilization matching. NO has been shown to cause arterial hyperpolarization, in part, via K_{ATP} channel activation (Murphy and Brayden, 1995) which may occur through the cGMP intermediary that elicits K_{ATP} channel activation in cardiac myocytes (Chai et al., 2011) and cultured smooth muscle cells (Kubo et al., 1994). Furthermore, as a reactive nitrogen species, NO can cause direct S-nitrosylation of cysteine residues found on the SURx subunit (Kawano et al., 2009; Yoshida et al., 2006), and channel activation via NO is likely mediated through a combination of the two mechanisms. The notion that K_{ATP} channels can act as an amplifier for NO and other vasoactive signals (Cole et al., 2000; Silva et al., 2008) via modulation of membrane potential deserves further investigation and may be valuable clinically (rev. by Akrouh et al., 2009).

Both the results herein and large retrospective studies of the association of sulphonylurea monotherapy with cardiovascular mortality and morbidity are cause for concern in diabetic and heart failure patients (Fadini et al., 2015; Morgan et al., 2014; Simpson et al., 2006). Our findings demonstrate the additive effect of GLI on PO_2mv dysregulation in heart failure which has been minimally addressed in the risk assessments of sulphonylurea therapy. The phase II muscle $\dot{V}O_2$ kinetics are significantly slowed in diabetic patients and an intriguing question is whether it is a diabetes- or sulphonlyurea-induced dysfunction of the K_{ATP} channel that is associated with the $\dot{V}O_2$ kinetics limitation (Bauer et al., 2007; O'Connor et al., 2015; Regensteiner et al., 1998). Clearly, when other pathways have been attenuated by heart failure the K_{ATP} channel remains one of the few defenses against a severe mismatch of O_2-delivery to O_2-utilization during contractions. The administration of sulphonylureas may pose a previously

unrecognized danger in patients afflicted with both heart failure and diabetes where an additional drag on O_2 delivery could bring physical activity to a halt.

Table 4-1. Morphological and hemodynamic characteristics of CHF rats.

	$\bar{X}$	$X(1) - X(n)$
LVEDP, mmHg	18 ± 1	10 – 27
LV dp/dt, mmHg/s	6270 ± 239	4900 – 8800
LV/body mass, mg/g	1.91 ± 0.03	1.73 – 2.07
RV/body mass, mg/g	0.59 ± 0.02	0.51 – 0.78
Lung/body mass, mg/g	3.56 ± 0.16	2.78 – 5.29
Infarct size, %	30 ± 1	18 - 42

Data are ± SEM. $\bar{X}$, sample mean; $X(1) - X(n)$, sample minimum to maximum; LVEDP, left ventricular end diastolic pressure; LV dp/dt, left ventricular dpressure/dtime RV, right ventricle; LV, left ventricle. $n = 16$

Table 4-2. Spinotrapezius PO_2mv parameters at rest and following the onset of contractions under control, GLI and PIN conditions.

	Control	GLI	PIN
$PO_2mv_{(BL)}$, mmHg	28.3 ± 0.9	24.8 ± 1.0*	32.5 ± 2.0$^{\#}$
Δ_1PO_2mv, mmHg	11.0 ± 0.7	9.7 ± 0.6*	9.7 ± 1.2
Δ_2PO_2mv, mmHg	2.3 ± 0.4	4.1 ± 0.5*	1.0 ± 0.4$^{\#}$
$PO_2mv_{(SS)}$, mmHg	19.6 ± 0.6	19.1 ± 0.9	23.8 ± 1.4$^{\#}$
TD_1, s	5.5 ± 0.9	4.7 ± 0.6	3.0 ± 0.7$^{\#}$
TD_2, s	39.0 ± 6.9	36.8 ± 5.2	57.0 ± 12.7
τ_1, s	10.6 ± 0.7	10.3 ± 1.0	16.8 ± 3.6
τ_2, s	33.6 ± 4.6	47.1 ± 5.4*	32.5 ± 7.2
MRT_1, s	16.2 ± 1.1	15.0 ± 1.0	19.8 ± 3.3
MRT_2, s	66.5 ± 9.4	83.9 ± 6.3*	89.5 ± 12.2
MRT_{Total}	66.1 ± 10.2	93.6 ± 7.8*	57.1 ± 14.1$^{\#}$

Values are mean ± SE. $PO_2mv_{(BL)}$, resting PO_2mv; Δ_1PO_2mv, amplitude of the first component; Δ_2PO_2mv, amplitude of the second component; $PO_2mv_{(SS)}$, contracting steady-state PO_2mv; TD_1, time delay of the first component; TD_2, time delay of the second component; τ_1, time constant of the first component; τ_2, time constant of the second component; MRT_1, mean response time of the first component; MRT_2, mean response time of the second component; MRT_{Total}, sum of the first and second component mean response times. One-component exponential model used for 11/16 control, 15/16 GLI and 11/12 PIN. All second component parameters calculated only from two-component models (control $n = 11$, GLI $n = 15$, PIN $n = 11$). * $p < 0.05$ vs. control. $^{\#}$ $p < 0.05$ vs GLI

Figure 4-1. Spinotrapezius PO_2mv profiles and kinetics representations.

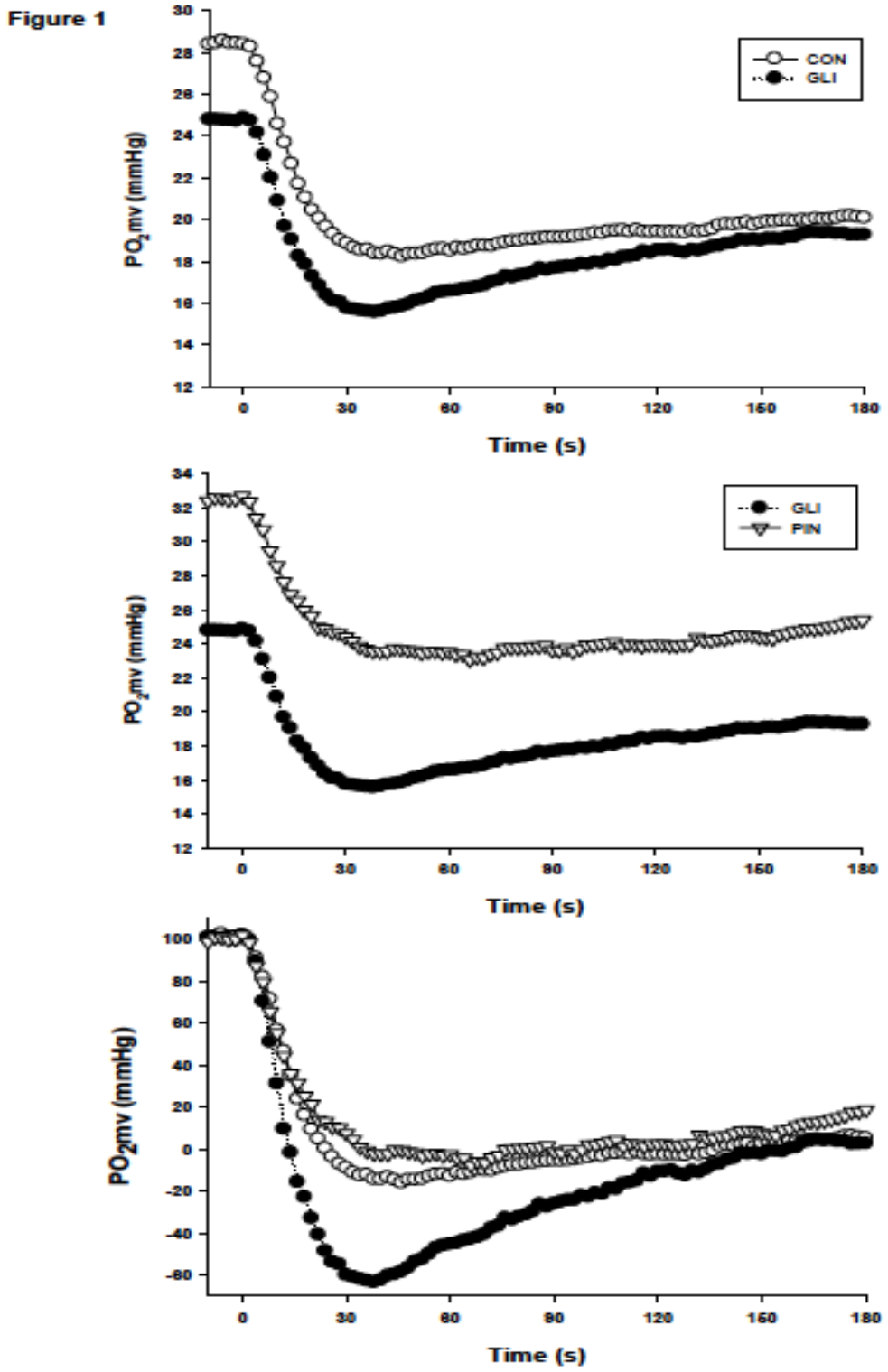

(Top panel) Absolute spinotrapezius PO_2mv profiles of control (open circles) vs GLI (closed circles) and (middle panel) GLI vs PIN (open triangle). 180 s of contractions began at time zero. (Bottom panel) Relative PO_2mv profiles of control, GLI and PIN.

References

Akrouh, A., Halcomb, S.E., Nichols, C.G., Sala-Rabanal, M., 2009. Molecular biology of KATP channels and implications for health and disease. IUBMB Life 61, 971–978.

Bailey, J.K., Kindig, C.A., Behnke, B.J., Musch, T.I., Schmid-Schoenbein, G.W., Poole, D.C., 2000. Spinotrapezius muscle microcirculatory function: effects of surgical exteriorization. Am. J. Physiol. Heart Circ. Physiol. 279, H3131–3137.

Banitt, P.F., Smits, P., Williams, S.B., Ganz, P., Creager, M.A., 1996. Activation of ATP-sensitive potassium channels contributes to reactive hyperemia in humans. Am. J. Physiol. 271, H1594–598.

Bank, A.J., Sih, R., Mullen, K., Osayamwen, M., Lee, P.C., 2000. Vascular ATP-Dependent Potassium Channels, Nitric Oxide, and Human Forearm Reactive Hyperemia. Cardiovasc. Drugs Ther. 14, 23–29.

Bauer, T.A., Reusch, J.E.B., Levi, M., Regensteiner, J.G., 2007. Skeletal muscle deoxygenation after the onset of moderate exercise suggests slowed microvascular blood flow kinetics in type 2 diabetes. Diabetes Care 30, 2880–2885.

Beech, D.J., Zhang, H., Nakao, K., Bolton, T.B., 1993. K channel activation by nucleotide diphosphates and its inhibition by glibenclamide in vascular smooth muscle cells. Br. J. Pharmacol. 110, 573–582.

Behnke, B.J., Barstow, T.J., Kindig, C.A., McDonough, P., Musch, T.I., Poole, D.C., 2002. Dynamics of oxygen uptake following exercise onset in rat skeletal muscle. Respir. Physiol. Neurobiol. 133, 229–239.

Behnke, B.J., Delp, M.D., Dougherty, P.J., Musch, T.I., Poole, D.C., 2005. Effects of aging on microvascular oxygen pressures in rat skeletal muscle. Respir. Physiol. Neurobiol. 146, 259–268.

Behnke, B.J., Kindig, C.A., Musch, T.I., Koga, S., Poole, D.C., 2001. Dynamics of microvascular oxygen pressure across the rest-exercise transition in rat skeletal muscle. Respir. Physiol. 126, 53–63.

Bijlstra, P.J., den Arend, J.A., Lutterman, J.A., Russel, F.G., Thien, T., Smits, P., 1996. Blockade of vascular ATP-sensitive potassium channels reduces the vasodilator response to ischaemia in humans. Diabetologia 39, 1562–1568.

Bodmer, S.I., Balestra, G.M., Harms, F.A., Johannes, T., Raat, N.J.H., Stolker, R.J., Mik, E.G., 2012. Microvascular and mitochondrial PO 2 simultaneously measured by oxygen-dependent delayed luminescence. J. Biophotonics 5, 140–151.

Chai, Y., Zhang, D.M., Lin, Y.F., 2011. Activation of cGMP-dependent protein kinase stimulates cardiac ATP-sensitive potassium channels via a ROS/calmodulin/CaMKII signaling cascade. PLoS One 6, e18191.

Chen, Y., Traverse, J.H., Zhang, J., Bache, R.J., 2001. Selective blockade of mitochondrial KATP channels does not impair myocardial oxygen consumption. Am. J. Physiol. Heart Circ. Physiol. 281, H738–H744.

Cole, W.C., Malcolm, T., Walsh, M.P., Light, P.E., 2000. Inhibition by protein kinase C of the K(NDP) subtype of vascular smooth muscle ATP-sensitive potassium channel. Circ. Res. 87, 112–117.

Copp, S.W., Ferreira, L.F., Herspring, K.F., Hirai, D.M., Snyder, B.S., Poole, D.C., Musch, T.I., 2009. The effects of antioxidants on microvascular oxygenation and blood flow in skeletal muscle of young rats. Exp. Physiol. 94, 961–971.

Delp, M.D., Duan, C., 1996. Composition and size of type I, IIA, IID/X, and IIB fibers and citrate synthase activity of rat muscle. J. Appl. Physiol. 80, 261–270.

Delp, M.D., Duan, C., Mattson, J.P., Musch, T.I., 1997. Changes in skeletal muscle biochemistry and histology relative to fiber type in rats with heart failure. J. Appl. Physiol. 83, 1291–1299.

Diederich, E.R., Behnke, B.J., McDonough, P., Kindig, C. a, Barstow, T.J., Poole, D.C., Musch, T.I., 2002. Dynamics of microvascular oxygen partial pressure in contracting skeletal muscle of rats with chronic heart failure. Cardiovasc. Res. 56, 479–486.

Duncker, D.J., Oei, H.H., Hu, F., Stubenitsky, R., Verdouw, P.D., 2001. Role of K(ATP)(+) channels in regulation of systemic, pulmonary, and coronary vasomotor tone in exercising swine. Am. J. Physiol. Heart Circ. Physiol. 280, H22–H33.

Dunphy, I., Vinogradov, S. a., Wilson, D.F., 2002. Oxyphor R2 and G2: Phosphors for measuring oxygen by oxygen-dependent quenching of phosphorescence. Anal. Biochem. 310, 191–198.

Fadini, G.P., Avogaro, A., Degli Esposti, L., Russo, P., Saragoni, S., Buda, S., Rosano, G., Pecorelli, S., Pani, L., Martinetti, S., Mero, P., Raeli, L., Migliazza, S., Dellagiovanna, M., Cerra, C., Gambera, M., Piccinelli, R., Zambetti, M., Atzeni, F., Valsecchi, V., DeLuca, P., Scopinaro, E., Moltoni, D., Pini, E., Leoni, O., Oria, C., Papagni, M., Nosetti, G., Caldiroli, E., Moser, V., Roni, R., Polverino, A., Bovo, C., Mezzalira, L., Andretta, M., Trentin, L., Palcic, S., Pettinelli, A., Arbo, A., Bertola, A., Capparoni, G., Cattaruzzi, C., Marcuzzo, L., Rosa, F. V., Basso, B., Saglietto, M., Delucis, S., Prioli, M., Filippi, R., Coccini, A., Ghia, M., Sanfelici, F., Radici, S., Scanavacca, P., Campi, A., Bianchi, S., Verzola, A., Morini, M., Borsari, M., Danielli, A., Dal Maso, M., Marsiglia, B., Vujovic, B., Pisani, M., Bonini, P., Lena, F., Aletti, P., Marcobelli, A., Sagratella, S., Fratini, S., Bartolini, F., Riccioni, G., Meneghini, A., Di Turi, R., Fano, V., Blasi, A., Pagnozzi, E., Quintavalle, G., D'Avenia, P., De Matthaeis, M.C., Ferrante, F., Crescenzi, S., Marziale, L., Venditti, P., Bianchi, C., Senesi, I., Baci, R., De Carlo, I., Lavalle, A., Trofa, G., Marcello, G., Pagliaro, C., Troncone, C., Farina, G., Tari, M.G., Motola, G., De Luca, F., Saltarelli, M.L., Granieri, C., Vulnera, M., Palumbo, L., La Viola, F., Florio, L., De Francesco, A.E., Costantino, D., Rapisarda, F., Lazzaro, P.L., Pastorello, M., Parlli, M., Visconti, M., Uomo, I., Sanna, P., Lombardo, F., 2015. Risk of hospitalization for heart failure in patients with type 2 diabetes newly treated with DPP-4 inhibitors or other oral glucose-lowering medications: a retrospective registry study on 127,555 patients from the Nationwide OsMed Health-DB Database. Eur. Heart J.

Farouque, H.M.O., Meredith, I.T., 2003. Effects of inhibition of ATP-sensitive potassium channels on metabolic vasodilation in the human forearm. Clin. Sci. (Lond). 104, 39–46.

Ferreira, L.F., Hageman, K.S., Hahn, S., Williams, J., Padilla, D.J., Poole, D.C., Musch, T.I., 2006a. Muscle microvascular oxygenation in chronic heart failure: role of nitric oxide availability. Acta Physiol. (Oxf). 188, 3–13.

Ferreira, L.F., Padilla, D.J., Williams, J., Hageman, K.S., Musch, T.I., Poole, D.C., 2006b. Effects of altered nitric oxide availability on rat muscle microvascular oxygenation during contractions. Acta Physiol. (Oxf). 186, 223–232.

Ferreira, L.F., Poole, D.C., Barstow, T.J., 2005. Muscle blood flow-O2 uptake interaction and their relation to on-exercise dynamics of O2 exchange. Respir. Physiol. Neurobiol. 147, 91–103.

Fishbein, M.C., Maclean, D., Maroko, P.R., 1978. Experimental myocardial infarction in the rat: qualitative and quantitative changes during pathologic evolution. Am. J. Pathol. 90, 57–70.

George, S., McBurney, A., Cole, A., 1990. Possible protein binding displacement interaction between glibenclamide and metolazone. Eur. J. Clin. Pharmacol. 38, 93–95.

Hepple, R.T., Liu, P.P., Plyley, M.J., Goodman, J.M., 1999. Oxygen uptake kinetics during exercise in chronic heart failure: influence of peripheral vascular reserve. Clin. Sci. (Lond). 97, 569–577.

Herspring, K.F., Ferreira, L.F., Copp, S.W., Snyder, B.S., Poole, D.C., Musch, T.I., 2008. Effects of antioxidants on contracting spinotrapezius muscle microvascular oxygenation and blood flow in aged rats. J. Appl. Physiol. 105, 1889–1896.

Hirai, D.M., Copp, S.W., Ferguson, S.K., Holdsworth, C.T., Musch, T.I., Poole, D.C., 2013. The NO donor sodium nitroprusside: evaluation of skeletal muscle vascular and metabolic dysfunction. Microvasc. Res. 85, 104–111.

Hirai, D.M., Copp, S.W., Holdsworth, C.T., Ferguson, S.K., McCullough, D.J., Behnke, B.J., Musch, T.I., Poole, D.C., 2014. Skeletal muscle microvascular oxygenation dynamics in heart failure: exercise training and nitric oxide-mediated function. Am. J. Physiol. Circ. Physiol. 306, H690–H698.

Hogan, M.C., Arthur, P.G., Bebout, D.E., Hochachka, P.W., Wagner, P.D., 1992. Role of O2 in regulating tissue respiration in dog muscle working in situ. J. Appl. Physiol. 73, 728–736.

Holdsworth, C.T., Copp, S.W., Ferguson, S.K., Sims, G.E., Poole, D.C., Musch, T.I., 2015. Acute blockade of ATP-sensitive K+ channels impairs skeletal muscle vascular control in rats during treadmill exercise. Am. J. Physiol. Heart Circ. Physiol. 11, H1434-H1442.

Kawano, T., Zoga, V., Kimura, M., Liang, M.Y., Wu, H.E., Gemes, G., McCallum, J.B., Kwok, W.M., Hogan, Q.H., Sarantopoulos, C.D., 2009. Nitric oxide activates ATP-sensitive potassium channels in mammalian sensory neurons: action by direct S-nitrosylation. Mol. Pain 5, 12.

Keller, D.M., Ogoh, S., Greene, S., Olivencia-Yurvati, A., Raven, P.B., 2004. Inhibition of KATP channel activity augments baroreflex-mediated vasoconstriction in exercising human skeletal muscle. J. Physiol. 561, 273–282.

Kubo, M., Nakaya, Y., Matsuoka, S., Saito, K., Kuroda, Y., 1994. Atrial natriuretic factor and isosorbide dinitrate modulate the gating of ATP-sensitive K+ channels in cultured vascular smooth muscle cells. Circ. Res. 74, 471–476.

Larsen, J.J., Dela, F., Madsbad, S., Vibe-Petersen, J., Galbo, H., 1999. Interaction of sulfonylureas and exercise on glucose homeostasis in type 2 diabetic patients. Diabetes Care 22, 1647–1654.

Miyazaki, A., Adachi, H., Oshima, S., Taniguchi, K., Hasegawa, A., Kurabayashi, M., 2007. Blood flow redistribution during exercise contributes to exercise tolerance in patients with chronic heart failure. Circ. J. 71, 465–470.

Morgan, C.L., Mukherjee, J., Jenkins-Jones, S., Holden, S.E., Currie, C.J., 2014. Association between first-line monotherapy with sulphonylurea versus metformin and risk of all-cause mortality and cardiovascular events: a retrospective, observational study. Diabetes. Obes. Metab. 16, 957–962.

Murphy, M.E., Brayden, J.E., 1995. Nitric oxide hyperpolarizes rabbit mesenteric arteries via ATP-sensitive potassium channels. J. Physiol. 486 Pt 1, 47–58.

Musch, T.I., Terrell, J. A., 1992. Skeletal muscle blood flow abnormalities in rats with a chronic myocardial infarction: rest and exercise. Am. J. Physiol. 262, H411–H419.

Nakai, T., Ichihara, K., 1994. Effects of diazoxide on norepinephrine-induced vasocontraction and ischemic myocardium in rats. Biol. Pharm. Bull. 17, 1341–1344.

O'Connor, E., Green, S., Kiely, C., O'Shea, D., Egaña, M., 2015. Differential effects of age and type 2 diabetes on dynamic vs. peak response of pulmonary oxygen uptake during exercise. J. Appl. Physiol. 118, 1031–1039.

Padilla, D.J., McDonough, P., Behnke, B.J., Kano, Y., Hageman, K.S., Musch, T.I., Poole, D.C., 2007. Effects of Type II diabetes on muscle microvascular oxygen pressures. Respir. Physiol. Neurobiol. 156, 187–195.

Piepoli, M.F., Guazzi, M., Boriani, G., Cicoira, M., Corrà, U., Dalla Libera, L., Emdin, M., Mele, D., Passino, C., Vescovo, G., Vigorito, C., Villani, G., Agostoni, P., 2010a. Exercise intolerance in chronic heart failure: mechanisms and therapies. Part II. Eur. J. Cardiovasc. Prev. Rehabil. 17, 643–648.

Piepoli, M.F., Guazzi, M., Boriani, G., Cicoira, M., Corrà, U., Dalla Libera, L., Emdin, M., Mele, D., Passino, C., Vescovo, G., Vigorito, C., Villani, G.Q., Agostoni, P., 2010b. Exercise intolerance in chronic heart failure: mechanisms and therapies. Part I. Eur. J. Cardiovasc. Prev. Rehabil. 17, 637–642.

Poole, D.C., Behnke, B.J., McDonough, P., McAllister, R.M., Wilson, D.F., 2004. Measurement of muscle microvascular oxygen pressures: compartmentalization of phosphorescent probe. Microcirculation 11, 317–326.

Poole, D.C., Hirai, D.M., Copp, S.W., Musch, T.I., 2012. Muscle oxygen transport and utilization in heart failure: implications for exercise (in)tolerance. Am. J. Heart Circ. Physiol. 302, H1050–H1063.

Regensteiner, J.G., Bauer, T.A., Reusch, J.E., Brandenburg, S.L., Sippel, J.M., Vogelsong, A.M., Smith, S., Wolfel, E.E., Eckel, R.H., Hiatt, W.R., 1998. Abnormal oxygen uptake kinetic responses in women with type II diabetes mellitus. J. Appl. Physiol. 85, 310–317.

Richardson, R.S., Noyszewski, E.A., Kendrick, K.F., Leigh, J.S., Wagner, P.D., 1995. Myoglobin O2 desaturation during exercise. Evidence of limited O2 transport. J. Clin. Invest. 96, 1916–1926.

Rumsey, W.L., Vanderkooi, J.M., Wilson, D.F., 1988. Imaging of phosphorescence: a novel method for measuring oxygen distribution in perfused tissue. Science 241, 1649–1651.

Sacre, J.W., Jellis, C.L., Haluska, B.A., Jenkins, C., Coombes, J.S., Marwick, T.H., Keske, M.A., 2015. Association of Exercise Intolerance in Type 2 Diabetes With Skeletal Muscle Blood Flow Reserve. JACC. Cardiovasc. Imaging 8, 913–921.

Sadraei, H., Beech, D.J., 1995. Ionic currents and inhibitory effects of glibenclamide in seminal vesicle smooth muscle cells. Br. J. Pharmacol. 115, 1447–1454.

Schrage, W.G., Dietz, N.M., Joyner, M.J., 2006. Effects of combined inhibition of ATP-sensitive potassium channels, nitric oxide, and prostaglandins on hyperemia during moderate exercise. J. Appl. Physiol. 100, 1506–1512.

Silva, K.E., Barbosa, H.C., Rafacho, A., Bosqueiro, J.R., Stoppiglia, L.F., Carneiro, E.M., Borelli, M.I., Del Zotto, H., Gagliardino, J.J., Boschero, A.C., 2008. INGAP-PP up-

regulates the expression of genes and proteins related to K+ATP channels and ameliorates Ca2+ handling in cultured adult rat islets. Regul. Pept. 148, 39–45.

Simpson, S.H., Majumdar, S.R., Tsuyuki, R.T., Eurich, D.T., Johnson, J.A., 2006. Dose-response relation between sulfonylurea drugs and mortality in type 2 diabetes mellitus: a population-based cohort study. CMAJ 174, 169–174.

Suzuki, M., Sasaki, N., Miki, T., 2002. Role of sarcolemmal K(ATP) channels in cardioprotection against ischemia/reperfusion injury in mice. J. Clin. Invest. 109, 509–516.

Tateishi, J., Faber, J.E., 1995. ATP-Sensitive K+ Channels Mediate 2D-Adrenergic Receptor Contraction of Arteriolar Smooth Muscle and Reversal of Contraction by Hypoxia. Circ. Res. 76, 53–63.

Thomas, G.D., Hansen, J., Victor, R.G., 1997. Atp-sensitive potassium channels mediate contraction- induced attenuation of sympathetic vasoconstriction in rat skeletal muscle. J. Clin. Invest. 99, 2602–2609.

Wheaton, W.W., Chandel, N.S., 2011. Hypoxia. 2. Hypoxia regulates cellular metabolism. Am. J. Physiol. Cell Physiol. 300, C385–C393.

Wilson, D.F., Erecińska, M., Drown, C., Silver, I.A., 1977. Effect of oxygen tension on cellular energetics. Am. J. Physiol. 233, C135–140.

Yoshida, T., Inoue, R., Morii, T., Takahashi, N., Yamamoto, S., Hara, Y., Tominaga, M., Shimizu, S., Sato, Y., Mori, Y., 2006. Nitric oxide activates TRP channels by cysteine S-nitrosylation. Nat. Chem. Biol. 2, 596–607.

Chapter 5 - Summary

The collection of studies herein describes the role of the vascular K_{ATP} channel in regulating skeletal muscle O_2 transport. The exploration includes varying exercise intensities, large muscle mass recruitment and discernment of fiber type heterogeneity across two powerful techniques that reflect spatial and temporal aspects of vascular control. Until now, the available data for K_{ATP} channel inhibition was limited by the redundancy of vasodilatory control and examined relatively benign exercise conditions. The characteristics of our exercise and disease (heart failure) paradigm investigated K_{ATP} channel function in a microenvironment likely to produce recruitment of the channel. The fiber type of the rat, the relative tissue hypoxia of heart failure and the greater demand on whole body oxygen utilization for treadmill running revealed previously unknown aspects of K_{ATP} channel function in matching skeletal muscle O_2 delivery to O_2 demand. Furthermore, the kinetics data presented a more complete description of this function by determining where the decrements in vascular function coincide with the exercise response which has been masked during steady-state investigations.

In a broad sense these results are expected to contribute to the evidence-based clinical treatment of diabetes. Given the pervasiveness of diabetes in Western society, the solution to the root problem of glucose regulation is often single-mindedly pursued. Our data complements the epidemiology demonstrating the cardiovascular risks of sulphonylureas and suggests that treatment approaches need to be carefully prescribed. Importantly, I posit that a focus on the function of the individual (e.g. work capacity) is the best starting point for clinical treatment because it would retain focus on the parallels between the indicators of disease severity and the most effective treatment (i.e. exercise and diet). This would prevent the costly mismanagement of pharmacological intervention in diabetes patients with tremendous dysfunction of the exercise

response across multiple systems. Despite these results the function of the K_{ATP} channel in vascular control has not been comprehensively addressed. Our results correct a deficiency in the literature by generating hypotheses for clinical investigations of sulphonylurea use in both diabetic populations and combined diabetes-heart failure patients. Comparison of novel data to our hemodynamic evidence of glibenclamide use will permit the appropriate interpretation of future study designs. Thus, many previously intractable questions of vascular K_{ATP} channel function in diabetes can now be meaningfully addressed.

I would like to acknowledge the contribution of the following co-authors to the work herein: Dr. Steven W. Copp, Dr. Scott K. Ferguson, Dr. Timothy I. Musch, Dr. David C. Poole, Trenton D. Colburn and Gabrielle E. Sims. Additionally, this work benefitted from the valuable technical assistance of the following individuals: K. Sue Hageman, Dr. Daniel M. Hirai, Michael J. White, Alex J. Fees, Dr. Inagaki Tadakatsu, and Jennifer L. Wright.